NTNU
Norwegian University of
Science and Technology

Development of Calculation Model for Heat Exchangers in Subsea Systems

Håkon Eriksen

Master of Science in Energy and Environment
Submission date: June 2010
Supervisor: Arne Olav Fredheim, EPT

Norwegian University of Science and Technology
Department of Energy and Process Engineering

Problem Description

1. Description of possible concepts for cooling of process streams in subsea systems
2. Review and description of methods for calculation of heat transfer and pressure drop for the fluid being cooled on the tubeside and for the seawater being heated on the outside of the tubes. Implementation of both natural and forced convection must be possible.
3. Establish a program system in Excel or Matlab for calculation of a complete seawater cooler. The program must allow for specification of necessary geometric parameters and stream data, and for implementation of thermo-physical data in table format by the user.
4. Carrying out simulation of two defined test cases (well stream cooling and compressor after-cooling)

Assignment given: 25. January 2010
Supervisor: Arne Olav Fredheim, EPT

Norges teknisk-
naturvitenskapelige universitet
NTNU
EPT-H-2010-14

Institutt for energi- og prosessteknikk

NTNU

MASTEROPPGAVE

for

Student Håkon Eriksen

Våren 2010

Etablering av beregnings modell for varmevekslere til kjøling av sub-sea strømmer

Development of calculation model for heat exchangers in sub-sea systems

Bakgrunn

Naturgass og olje som produseres transporteres vanligvis via rørledning til en plattform for videre behandling før produktene transporteres til markedet. Mange av de nye feltene som utvikles i dag har en størrelse og plassering som gjør at bruk av undervannsanlegg kan gi økonomiske fordeler i forhold til bruk av plattformløsninger.
I forbindelse med undervanns prosessering vil en ofte ha behov for kjøling av fluidet i kontrollerte former. Dette kan være kjøling av brønnstrøm inn mot et prosessanlegg for å felle ut væske eller kjøling av resirkulasjonsgass i forbindelse med kompresjon av gass.
Forskjellige konsept for sub-sea varmevekslere er utviklet. Flere av disse er åpne rør-varmevekslere som baserer seg på naturlig konveksjon på utside av rørene. Det omliggende sjøvannet benyttes som kjølemedium. Slike system har utfordringer knyttet til kontroll av temperatur på rørside fluidet. I dag finnes det ingen tilgjengelige modeller for termisk-hydraulisk design av slike varmevekslere.

Mål

Målet for oppgaven er å etablere et programsystem for simulering av sjøvannskjølere. Det skal kunne simuleres både åpne, semi-åpne og lukkede varmevekslere. Programmet skal baseres på rørkjølere med variable antall rør i parallell. Det forutsettes at termo-fysikalske data er gitt på forhånd og ikke beregnes som del av programmet.

Oppgaven bearbeides ut fra følgende punkter:

1. Beskrivelse av mulige konsept for kjøling av prosesstrømmer i et sub-sea anlegg.

2. Gjennomgang og beskrivelse av metoder for beregning av varmeovergang og trykkfall for fluidet som kjøles på rørside samt for sjøvann som varmes opp på utside av rør. Både naturlig og tvungen konveksjon må kunne implementeres.

3. Etablering av et programsystem i excel eller Matlab for beregning av en komplett sjøvannskjøler. Nødvendige geometriske parametre og strømdata må kunne spesifiseres og termo-fysikalske data må kunne implementeres i tabell format av bruker. Varmeovergangstall og trykkfall må enten kunne spesifiseres eller beregnes fra modeller.

4. Gjennomføring av simulering for to definerte test case (brønnstrømskjøling og gass resirkulasjonskjøling)

-- " --

Senest 14 dager etter utlevering av oppgaven skal kandidaten levere/sende instituttet en detaljert fremdrift- og evt. forsøksplan for oppgaven til evaluering og evt. diskusjon med faglig ansvarlig/ veiledere. Detaljer ved evt. utførelse av dataprogrammer skal avtales nærmere i samråd med faglig ansvarlig.

Besvarelsen redigeres mest mulig som en forskningsrapport med et sammendrag både på norsk og engelsk, konklusjon, litteraturliste, innholdsfortegnelse etc. Ved utarbeidelsen av teksten skal kandidaten legge vekt på å gjøre teksten oversiktlig og velskrevet. Med henblikk på lesning av besvarelsen er det viktig at de nødvendige henvisninger for korresponderende steder i tekst, tabeller og figurer anføres på begge steder. Ved bedømmelsen legges det stor vekt på at resultatene er grundig bearbeidet, at de oppstilles tabellarisk og/eller grafisk på en oversiktlig måte, og at de er diskutert utførlig.

Alle benyttede kilder, også muntlige opplysninger, skal oppgis på fullstendig måte. (For tidsskrifter og bøker oppgis forfatter, tittel, årgang, sidetall og evt. figurnummer.)

Det forutsettes at kandidaten tar initiativ til og holder nødvendig kontakt med faglærer og veileder(e). Kandidaten skal rette seg etter de reglementer og retningslinjer som gjelder ved StatoilHydro og alle (andre) fagmiljøer som kandidaten har kontakt med gjennom sin utførelse av oppgaven, samt etter eventuelle pålegg fra Institutt for energi- og prosessteknikk.

I henhold til "Utfyllende regler til studieforskriften for teknologistudiet/sivilingeniørstudiet" ved NTNU § 20, forbeholder instituttet seg retten til å benytte alle resultater i undervisnings- og forskningsformål, samt til publikasjoner.

Ett -1 komplett eksemplar av originalbesvarelsen av oppgaven skal innleveres til samme adressat som den ble utlevert fra. (Det skal medfølge et konsentrert sammendrag på maks. en maskinskrevet side med dobbel linjeavstand med forfatternavn og oppgavetittel for evt. referering i tidsskrifter).
Til Instituttet innleveres to - 2 komplette, kopier av besvarelsen. Ytterligere kopier til evt. medveiledere/oppgavegivere skal avtales med, og evt. leveres direkte til, de respektive.
Til instituttet innleveres også en komplett kopi (inkl. konsentrerte sammendrag) på CD-ROM i Word-format eller tilsvarende.

Institutt for energi og prosessteknikk, 5 januar 2010

Olav Bolland
Instituttleder

Arne O. Fredheim
Faglærer/veileder

Medveileder: Knut Maråk (Statoil)

Preface

This master thesis is written during the tenth and final semester of the Master of Science studies in Energy and environmental engineering, at the department of energy and process engineering, NTNU.

The purpose of this work is to develop a calculation model for a subsea heat exchanger.

I would like to thank my supervisor Arne Olav Fredheim for the guidance through the period of this study. In addition I would like to thank Erling Næss for discussions around heat transfer, Ole-Jørgen Nydal for discussions around two-phase flow and Knut Arild Maråk for helping me with various topics.

Trondheim, June 2010

Håkon Eriksen

Abstract

Subsea processing can make production from otherwise unprofitable fields profitable. In subsea processing controlled cooling of the process fluid will often be required. Robust and simple solutions are desirable in subsea processing. Coolers that rely on natural convection from the surrounding seawater are therefore interesting, but control of the process fluid outlet temperature is hard to obtain in such coolers.

In this study a calculation model for subsea coolers has been developed. The commercial software MATLAB has been used for developing a program. Heat transfer and frictional pressure drop correlations have been studied and recommendations are made for the model. The model is based on tubes in parallel, and the tubes can be oriented vertically or horizontally. The program allows for open, semi-open and closed arrangements on the waterside, and both natural and forced convection is implemented.

The program has been tested through simulations of two test cases and found to be performing as desired.

Table of Contents

Nomenclature

A	area (m^2)
c_p	isobaric specific heat capacity (J/kgK)
C	empirical constant in Lockhart-Martinelli correlation
C_f	Two-phase enhancement factor
D	diameter (m)
e	equivalent sand corn roughness (m)
E	parameter in Friedel's correlation
f	friction factor, two-phase enhancement factor
F	parameter in Friedel's correlation
Fr	Froude number
G	mass flux (kg/m^2s)
g	gravity constant (m/s^2)
Gr	Grashof number
h	enthalpy (J/kg)
H	parameter in Friedel's correlation
k_α	Correction factor for Boyko and Kruzhilin's correlation
l	length (m)
m	mass flow rate (kg/s)
Nu	Nusselt number
P	pressure (bar, Pascal), wetted perimeter (m)
Pr	Prandtl number
Q	duty (W)
q	heat flux (W/m^2)
R	thermal resistance (K/W)
Ra	Rayleigh number
Re	Reynolds number
S	slip ratio
T	temperature (K)
U	overall heat transfer coefficient (W/m^2K)
v	velocity (m/s)
We	Weber number
x	vapor mass fraction, distance(m)
X	parameter in Lockhart-Martinelli correlation
Y	parameter in Chisholm's correlation
z	longitudinal coordinate (m)
Z_g	ratio between sensible and total heat flux

Greek symbols

α	heat transfer coefficient (W/m^2K)
β	volume expansion coefficient (K^{-1})
δ	film thickness (m)

ε	void fraction
λ	thermal conductivity (W/mK)
μ	dynamic viscosity (Ns/m^2)
ρ	density (kg/m^3)
σ	surface tension (N/m)
τ	shear stress (N/m^2)
υ	kinematic viscosity (m^2/s)
ψ	two-phase enhancement factor in Fuchs' correlation
ϕ	two-phase friction multiplier

Subscripts

acc	acceleration
c	characteristic
o	outer, external
i	internal, interfacial
f	fouling
film	liquid film
fric	frictional
g	gas
go	gas only
gs	gas superficial
h	homogenous
max	maximum
min	minimum
l	liquid
lo	liquid only
sp	single phase
tp	two phase
v	vapor
w	wall

List of figures

List of tables

1 Introduction

Subsea processing can make oil and gas production from remote or small fields more profitable. Subsea processing is currently under development and new solutions are being developed continuously. An example of subsea processing is compression of the gas in order to maintain a production level. Another example is cooling of the well stream for separation of heavier hydrocarbons and separation and injection of water. In order to achieve the desired results in the mentioned examples, controlled cooling of the fluid may be necessary. If the surrounding seawater is used as coolant the control can be hard to achieve.

The aim of this study is to develop a calculation model for a subsea heat exchanger for cooling. The calculation model is relevant for a cooler with tubes in parallel, and includes both passive cooling, which utilizes natural convection or the natural motion of the seawater, and active cooling, which uses forced convection from circulating water. The commercial software MATLAB is used for implementing the model.

The report starts with a review of possible concepts for cooling of process streams in a subsea processing facility. It continues with theory for calculation of heat transfer on the outside and inside of tubes, in addition to calculation of pressure drop on the inside. Heat exchanger theory is then presented, before the implementation in MATLAB is described. The calculation model is used on one case study on well-stream cooling, and on one case study on after-cooling of gas from a compressor. Results and discussions around the result are presented. Conclusions and suggestions for further work on the calculation model are discussed finally.

2 Heat exchangers in subsea processing

2.1 Anti surge/ gas recycle

In order to maintain a production level from a field with decreasing wellhead pressure, subsea compression can be an option. In any compression solution a recycle bypass is desirable. The recycle loop is important in order to keep a minimum flow through the compressor for avoiding a surge situation. Surge is an unstable flow situation that occurs when the pressure at the outlet of the compressor becomes to high so that some gas flows backwards through the compressor. Figure 2.1-1 shows a principal sketch of a compressor with a gas recycle loop.

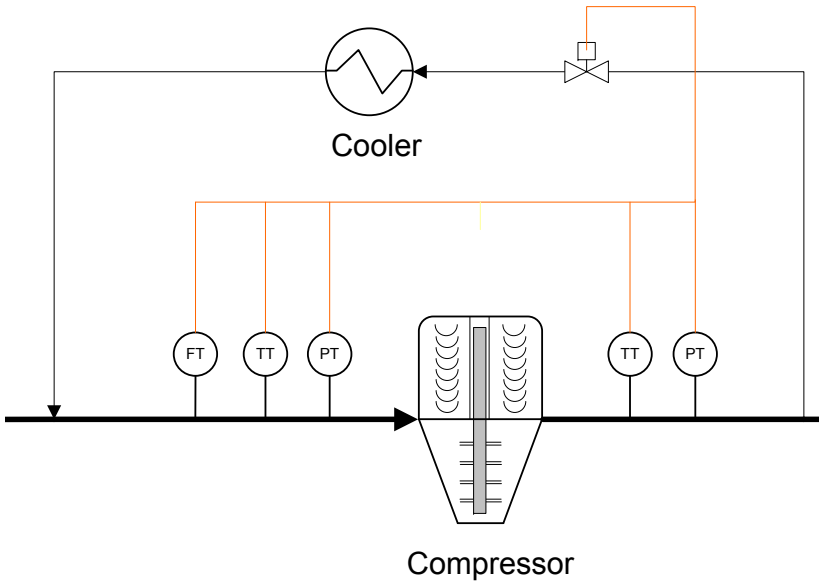

Figure 2.1-1 Compression with gas recycle and cooler [1]

Because of the energy input to the gas through the compressor the temperature of the gas increases. The recycled gas must be cooled in order to maintain the desired inlet temperature to the compressor. The compressor performance is better at lower temperatures because the density of the gas decreases with increasing temperature.

2.2 Well stream cooler

Figure 2.2-1 shows a conventional subsea boosting solution.

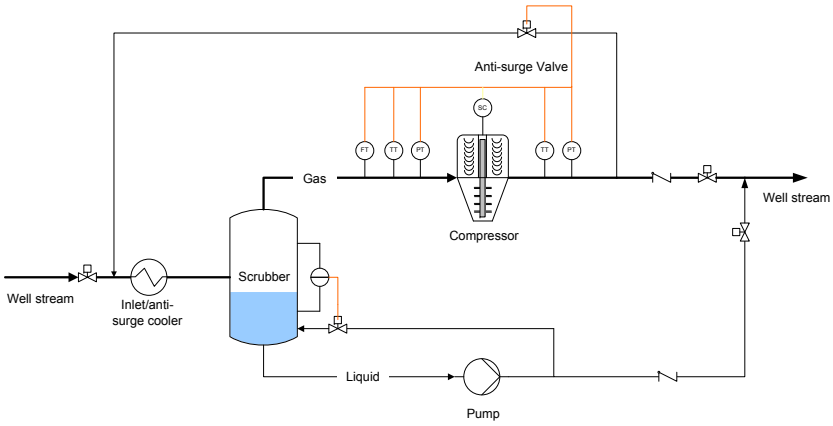

Figure 2.2-1 Conventional gas compression system [1]

Both the recycled gas and the well stream are cooled in a combined anti-surge and inlet cooler. In general this can also be done in two separate coolers. The liquid formed in the cooler is separated in the scrubber and sent to the pump, while the gas goes to the compressor before the two streams are mixed together for transportation in a multiphase pipeline to a platform or an onshore installation.

2.3 Important aspects in subsea cooling

Outlet temperature on the cooler, whether it is a well stream cooler or an anti-surge cooler, is crucial to control. If the outlet temperature of the well-stream cooler is too high liquid may form in the compressor because of unsatisfying separation and the performance of the compressor is reduced and it might also break down. And if the outlet temperature of the anti-surge cooler becomes too high the compressor performance is also reduced because the inlet temperature rises. On the other hand if the temperature becomes too low hydrates can form. Hydrates are solids of hydrocarbons and water that can form when free water is present in the well stream. At what conditions hydrates form is dependant on well stream composition, temperature, pressure and the existence of free water. The formation of hydrates is crucial to avoid.

It is also common to place an after-cooler after the compressor. The after-cooler cools the gas in order to increase the density of the mixture so that more fluid can be transported through the pipeline. The specifications for an after-cooler are for pipeline transport.

Good calculation models for subsea heat exchangers plays a very important role when designing a subsea processing facility.

3 Concepts for subsea cooling

Several companies design and produce subsea solutions and components, but public information about the heat exchanger solutions used for subsea coolers is difficult to find. A thorough search of the web and Science Direct has been carried out. Possible solutions will be presented in this chapter. Two patents exist at the World Intellectual Property Organization (WIPO). These two will be presented here along with some basic solutions.

3.1 Passive parallel tube cooler

Since the cooling capacity is basically infinite at the sea bottom it seems convenient to expose the fluid carrying tubes to seawater and rely on natural and forced convection from the seawater. In order to increase the heat transfer surface and decrease the pressure drop the flow should be divided into several parallel tubes. This is known as a passive cooler because it uses no external means for circulating the seawater.

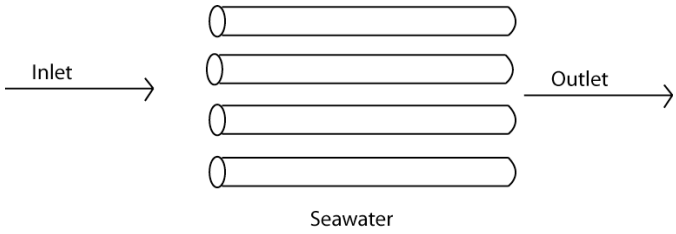

Figure 3.1-1 Open parallel tube cooler

Figure 3.1-1 shows a birds view of a principal sketch of a parallel tube cooler. In reality these tubes will have bends in order to make the design more compact. This is the simplest kind of heat exchanger. When designing a subsea processing facility it is desirable to make the design robust and simple. In that respect the passive parallel tube cooler is advantageous. On the other hand, the disadvantage is that it is difficult to control the outlet temperature. If there are currents in the seawater the heat transfer rate can increase significantly and the temperature may become too low. If the rest of the subsea processing facility is very reliant on a specific outlet temperature from the cooler this design can cause operational difficulties.

If there is no current in the surrounding seawater poor heat transfer can be experienced. This leads to increased area requirements in the heat exchanger. In order to make the heat exchanger more compact, finned tubes can be used for increasing the heat transfer area. A finned tube is illustrated in Figure 3.1-2

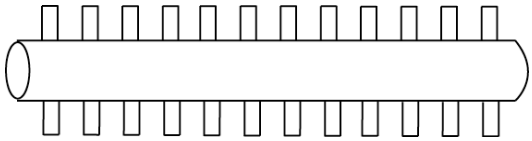

Figure 3.1-2 Finned tube

3.2 Subsea shell and tube

A well-known type of heat exchanger is the shell and tube heat exchanger. It consists of many parallel tubes with a shell wrapped around the tubes. The flow on the shell-side can be organized in many ways. Figure 3.2-1 shows an illustration of one kind of shell and tube heat exchanger. This type of heat exchanger is the most commonly used heat exchanger in onshore processes. It is robust, and a lot of research has been done on it. Based on this it seems promising to used this kind of heat exchanger subsea as well.

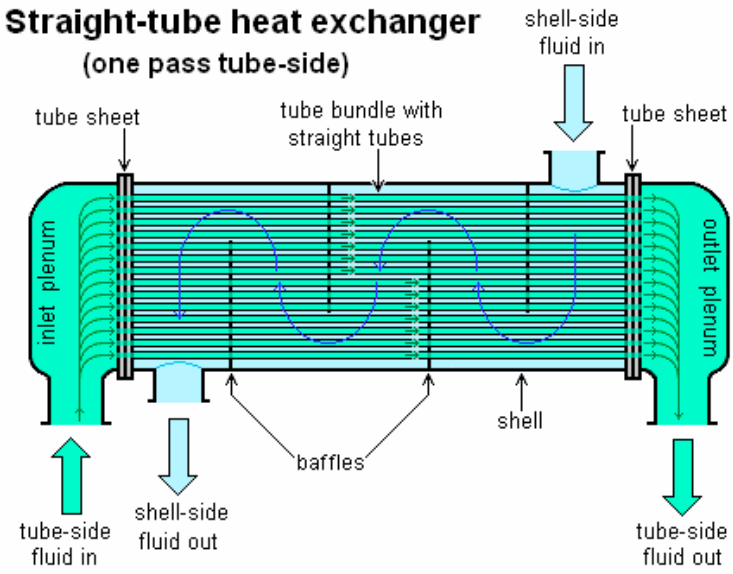

Figure 3.2-1 Shell and tube heat exchanger[2]

This is an active cooler, which needs an external pump for circulating the coolant on the shell-side. The coolant can be seawater, but also other coolants can be used if the heat exchanger is connected to a platform for example. Good calculation models and software exist for this kind of heat exchanger, which is an advantage. An additional disadvantage to the external pump is the material costs. The shell needs to withstand the high

static pressure of the surrounding seawater if other coolants than the seawater are used.

3.3 Subsea heat exchanger

At WIPO a patent is registered for a subsea cooler that uses convection from the surrounding water to cool the fluid [**3**]. The purpose of this heat exchanger is to control the velocity of the seawater in order to control outlet conditions. Figure 3.3-1 shows an illustration of the heat exchanger.

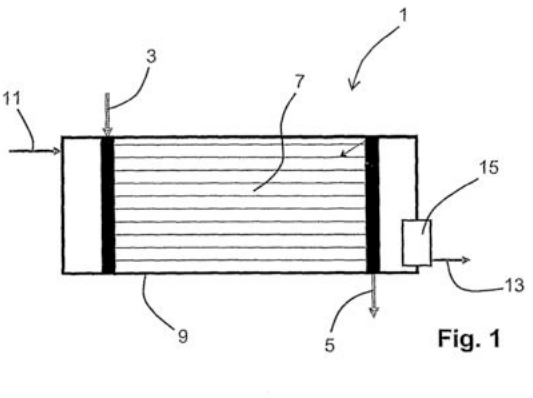

Figure 3.3-1 Convection heat exchanger (Aker Subsea AS) [3]

The hot fluid inlet is at (3) and outlet at (5). The seawater inlet is at (11) and seawater outlet at (13). The fluid carrying tubes (7) are in direct contact with the seawater. The tubes are confined in an enclosure (9). A pump (15) is placed at the seawater outlet for generating motion in the seawater.

The pump enables the operator to control the flow of the seawater and hence the outlet temperature of the tube-side fluid. The heat exchanger is hydrostatically balanced with the surrounding seawater. The only pressure difference is that caused by the pump. This facts gives the advantages that the walls of the heat exchanger does not have to sustain a big pressure difference and the motor for the pump does not have to be big. In the case that no cooling is desirable the pump can be turned off and the seawater inside the enclosure will reach the process fluid temperature, and act as insulation.

The obvious disadvantage here is the need for a motor and a pump. The motor and pump solution must be designed so that no leakages can penetrate into the motor. The inventor also describes a solution without a pump. If the arrangement of the heat exchanger is in such a way that the seawater flow is vertical the temperature rise of the seawater can be utilized. As the seawater flows through the convections section it gets heated. This leads to a density difference from seawater outlet to inlet. This density difference gives a pressure difference. The flow of seawater can then be controlled with a valve at the seawater inlet or outlet.

3.4 Subsea cooler with propeller

At WIPO another patent is registered for a subsea cooler. This patent [**4**] is for a heat exchanger that uses a propeller for generating fluid motion around the fluid carrying tubes. Figure 3.4-1 shows a principal sketch of the heat exchanger.

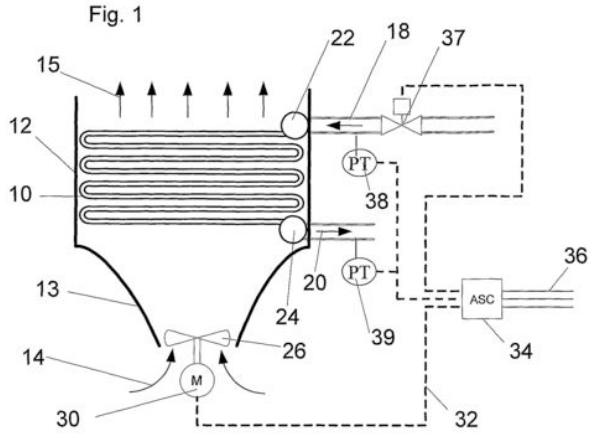

Figure 3.4-1 Principal sketch of subsea cooler with propeller (FMC Kongsberg Subsea AS) [4]

The hot fluid inlet is at (18) and outlet at (20). The tube arrangement (10) can consist of many tubes in parallel. A distribution unit (22) is placed at the inlet, and a gathering unit (24) at the outlet.

The purpose of the invention is to increase the flow of seawater past the tubes by the means of a propeller. The propeller (14) is rotated by power from the motor (30). The controller (34) regulates the motor, which generates the desired velocity of the seawater, which in turn controls the outlet temperature of the process fluid. In order to enhance the cooling effect an open-ended duct (12) is placed around the tubes. The seawater is then forced to flow past the tubes.

This invention also needs external power to drive the motor for the propeller. The inventor suggests several solutions for generating some of the required power from the energy of the process fluid. One of these solutions is illustrated in Figure 3.4-2.

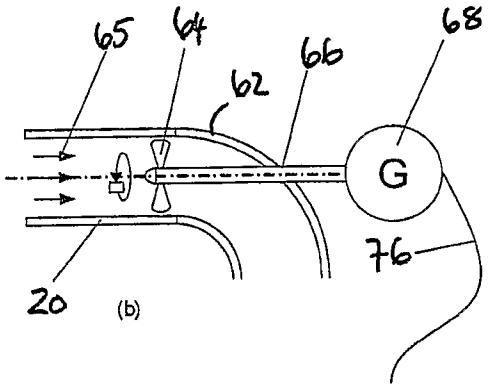

Figure 3.4-2 Power generation from process fluid [4]

The process fluid goes through a propeller (64) after the outlet, causing this propeller to rotate. The propeller is connected to a shaft (66), which is connected to a generator (68). The energy taken out from the fluid must be of course be added in the compressor again, so if the heat exchanger is part of a compressor solution this solution has no energy savings. But it could have area savings because of the increased heat transfer.

3.5 Ongoing projects on subsea coolers

There are two master theses on subsea coolers at the Norwegian University of Science and Technology (NTNU), in addition to this study. One of them is a study on natural convection around tubes by computational fluid dynamics (CFD) modeling. The other one is an experimental study for investigating heat transfer coefficients in natural convection. At the University in Oslo (UiO) there is a research project with a doctor degree. The project is both an experimental and numerical investigation of heat transfer in natural convection for subsea heat exchangers. The results of the three mentioned projects will be interesting to follow.

4 Theoretical background

4.1 Introduction

Good estimation of heat transfer and pressure drop are crucial in any heat exchanger design. In this chapter, methods for estimating heat transfer and pressure drop inside tubes will be discussed. Both single phase and condensation heat transfer will be reviewed. In addition, methods for estimating heat transfer on the outside of tubes will be discussed. Both natural and forced convection heat transfer will be examined.

4.2 Flow pattern

Some methods use flow pattern for basis of calculation of pressure drop and heat transfer. In order to decide pressure drop and heat transfer in such methods knowledge of flow-pattern is required. The different flow patterns that can be experienced during condensation inside horizontal tubes are illustrated in Figure 4.2-1 from El Hajal et al [**5**].

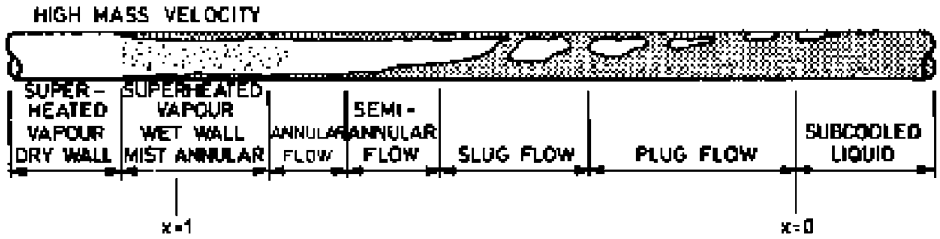

Figure 4.2-1 Flow patterns during condensation inside horizontal tubes [5**]**

Numerous flow pattern maps have been proposed for predicting flow pattern in two-phase flow. El Hajal et al [**5**] proposed a new flow pattern map for condensation based on a flow pattern map developed by Kattan et al [**6**] for flow boiling. Figure 4.2-2 shows the flow pattern map for R-134 at 40 C in 8 mm tubes. A denotes annular flow, I intermittent, SW stratified wavy, S stratified and MF mist flow.

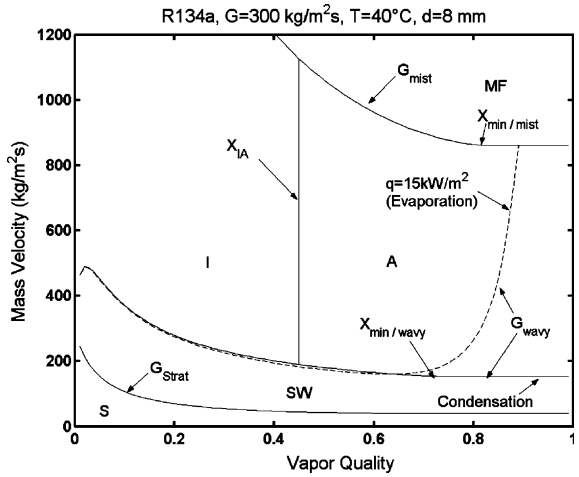

Figure 4.2-2 Map illustrating transition boundaries between the flow patterns [5]

The map in Figure 4.2-2 is only valid for the mentioned fluid at the given conditions and is only meant as an illustration. The transition boundaries must be calculated for the actual fluid and conditions. The method for calculating these boundaries is presented in [**5**].

4.3 Single phase frictional pressure drop

Total pressure drop consists of three components, namely frictional pressure drop, acceleration or momentum pressure drop, and gravitational pressure drop. This section deals with single-phase frictional pressure drop.

4.3.1 Definition of friction factor and Reynolds number

The friction factor is a dimensionless parameter used for deciding frictional pressure drop. It is defined as

$$f = \frac{8\tau_w}{\rho v^2}$$

Equation 4.3-1

or

$$f = \frac{(-\frac{dp}{dz_{fric}})}{\rho v^2 / (2D)}$$

Equation 4.3-2

The friction factor is a function of geometry, surface roughness and Reynolds number. The Reynolds number is the ratio of inertia forces to viscous forces and is defined as:

$$\mathrm{Re} = \frac{\rho v l_c}{\mu}$$

Equation 4.3-3

Where l_c is the characteristic length and defined as the tube diameter for single-phase flow in tubes. For laminar flow in tubes, the friction factor is defined as

$$f = \frac{64}{\mathrm{Re}}$$

Equation 4.3-4

The transition to turbulent flow is at Reynolds number at 2300. The accepted formula for the friction factor for turbulent flow in smooth tubes is [**7**]:

$$\frac{1}{f^{1/2}} = 2.0 \log(\mathrm{Re}\, f^{1/2}) - 0.8$$

Equation 4.3-5

Equation 4.3-5 is implicit but several alternative explicit approximations exist. That of Blasius is widely used, but is only valid for Reynolds numbers up to 100 000.

4.3.2 Effect of rough walls

Rough walls increase the frictional pressure drop. Colebrook suggested a formula that covers both smooth and rough tubes. The formula is an interpolation between Equation 4.3-5 and an expression for fully rough flow and can be used for the whole range. The formula is given as [**7**].

$$\frac{1}{f^{1/2}} = -2.0 \log\left(\frac{e/D}{3.7} + \frac{2.51}{\mathrm{Re}\, f^{1/2}}\right)$$

Equation 4.3-6

Where e is the equivalent sand corn roughness. Equation 4.3-6 is implicit, but Haaland [**8**] proposed an alternative explicit formula that deviates maximum only 2 percent from Equation 4.3-6 [**7**]. The explicit formula is given as

$$\frac{1}{f^{1/2}} = -1.8 \log\left(\left(\frac{e/D}{3.7}\right)^{1.11} + \frac{6.9}{\mathrm{Re}}\right)$$

Equation 4.3-7

4.4 Tube side single phase heat transfer coefficient

4.4.1 Definition of heat transfer coefficient and Nusselt number

The heat transfer coefficient (HTC) is the ratio between heat flux and the temperature difference between the bulk fluid and the tube wall, and is defined by Equation 4.4-1.

$$\alpha = \frac{q}{(T_b - T_w)}$$

Equation 4.4-1

It is common to group variables into dimensionless groups in order to reduce the number of variables. The heat transfer coefficient nondimensionalized is known as the Nusselt number. Equation 4.4-2 defines the Nusselt number.

$$Nu = \frac{\alpha l_c}{\lambda}$$

Equation 4.4-2

The Nusselt number can be interpreted as the ratio between convective heat transfer to conductive heat transfer. The characteristic length for single-phase heat transfer inside tubes is the tube diameter.

4.4.2 Single-phase heat transfer coefficient

In heat exchanger design it is important with good predictions of heat transfer coefficients for single-phase flow. Also for prediction of condensation heat transfer, because single phase HTCs are used.

Single-phase HTCs are usually expressed as a function of Reynolds number and Prandtl number. The Prandtl number account for physical properties of the fluid and can be interpreted as the ratio of momentum diffusivity to thermal diffusivity and is defined as:

$$\mathrm{Pr} = \frac{\mu c_p}{\lambda}$$

Equation 4.4-3

A simple and often used correlation for single phase HTC is that of Dittus-Boelter. Equation 4.4-4 gives the expression for cooling. It is valid for Prandtl numbers between 0.7 and 60 and Reynolds numbers above 10 000 (fully developed turbulent flow).

$$Nu = 0.023 \mathrm{Re}^{0.8} \mathrm{Pr}^{0.3}$$
Equation 4.4-4

Equation 4.4-4 may give errors as large as 25 % [**9**]. A more accurate correlation is proposed by Gnielinski [**10**]. He used the work of Pethukov [**11**] and expanded the correlation into the transition area between laminar and turbulent flow. This correlation is the most used and is suggested by the Heat Exchanger Design Handbook [**12**]. It is expressed as:

$$Nu = \frac{(f_{smooth} / 8)(\mathrm{Re} - 1000)\mathrm{Pr}}{1 + 12.7(f_{smooth} / 8)^{0.5}(\mathrm{Pr}^{2/3} - 1)}$$
Equation 4.4-5

The friction factor should be determined from an appropriate correlation for smooth tubes (i.e. Equation 4.3-5). The correlation is valid for Reynolds numbers from 2000 to 5 000 000, and Prandtl numbers from 0.5 to 2000.

4.4.3 Effect of rough surfaces

Surface roughness disturbs the laminar sublayer where most of the resistance against heat transfer is (for liquids with Prandtl numbers > 0.6). Hence, rough surfaces improve heat transfer. Norris [**13**] proposes the following correction for the affect of surface roughness on heat transfer:

$$\frac{Nu}{Nu_{smooth}} = \left(\frac{f}{f_{smooth}}\right)^n$$
Equation 4.4-6

where $n=0.68\mathrm{Pr}^{0.215}$. For $f/f_{smooth} > 4$ the HTC no longer increases. f is calculated from Equation 4.3-7 and f_{smooth} from Equation 4.3-5.

4.5 Pure component condensation heat transfer

4.5.1 Introduction

Condensation heat transfer is closely linked with flow pattern. In condensation of pure component one assumes that the vapor is saturated, so that all the resistance against heat transfer is in the liquid that is formed. If the liquid film formed is laminar Nusselt's theory [**14**] yields, and the heat transfer is governed by the conductivity of the liquid film and the film thickness. But at high mass velocities a substantial interfacial shear will be present. The interfacial shear induces turbulence in the liquid film so that convective effects will govern the heat transfer.

Different models exist for prediction of convective condensation for pure components. Some use a two-phase multiplier and a single-phase liquid

heat transfer correlation, some take use of the interfacial shear force which in turn requires knowledge of a frictional pressure gradient, and some use a flow pattern based approach. Three different models, representing each of the mentioned alternatives will be presented.

Annular flow (see Figure 4.2-1) will be the most commonly experienced flow pattern in the present study because of high mass velocities and high vapor mass fractions, so the focus will be on heat transfer in annular flow.

4.5.2 Two-phase heat transfer correlations

Three correlations have been looked at:

- The Heat Exchanger design handbook (HEDH) correlation[**12**]
- The modified Boyko and Kruzhilin correlation [**15**]
- Thome's correlation[**16**]

The three correlations and the basic data are described in appendix A. The HEDH correlation is chosen because it is a renowned source and the handbook is commonly used in heat exchanger design. The modified Boyko and Kruzhilin correlation is interesting because the modification is made based on experiments with high-pressure hydrocarbons. Thome's correlation is based on a database of results from experiments with hydrocarbons and refrigerants, and has a minimum of empirically determined constants.

4.5.3 Comparison of correlations for heat transfer

Figure 4.5-1 shows a comparison between the three mentioned correlations for the fluid and flow situation described in appendix C. The fluid used here is not a single component fluid, but only the liquid film HTC is shown here. The correlation from Thome et al deviates significantly from the others between vapor fractions of 0.3 and up. For this particular fluid the thermal conductivity of the liquid varies a lot as function of mass fraction. This is clearly seen in the HTC predicted by the Thome correlation, which is more dependent on the liquid thermal conductivity than the other. The correlation from Boyko and Kruzhilin is more dependent on the mass fraction and the density ratio. While the HEDH correlation is very dependant on the interfacial shear force.

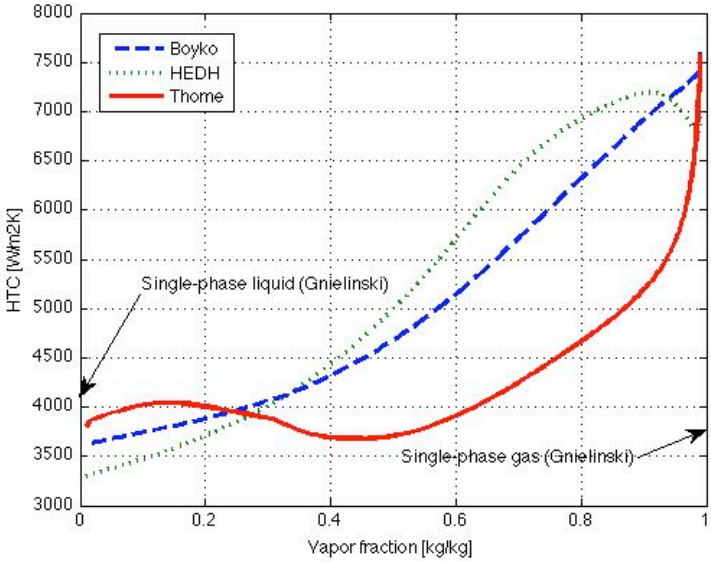

Figure 4.5-1 Liquid film heat transfer coefficient

From Thome et al [**16**] one can see that the correlation gives good accuracy to the values from refrigerants in the database, 85% of the data points (1850 points) lies within 20% of the predicted HTCs. But for hydrocarbons (921 points) it only predicts 55% of the HTCs within 20%. If the fact that it deviates from the other correlations mentioned here also is taken into account, this correlation seems uncertain. The Thome correlation is closest to the single-phase liquid HTC at x=0.

The Boyko and Kruzhilin correlation is a complete theoretical model [**15**], which makes it interesting if it accounts for all the effects. The fact that it uses a liquid only HTC ensures that it will have a smooth transition as x approaches zero. But with the correction factor proposed by Neeraas it "hits" x equal to zero 13% (1-1/1.15) below the single-phase liquid HTC. Neeraas found that the Boyko and Kruzhilin correlation with his correction gave good agreement to his experiments with propane. Only one of the 38 points in the experiments deviates with more than 10% from the modified correlation.

The HEDH does not mention what data the correlation is based on. But it seems to predict relatively similar values to the corrected Boyko and Kruzhilin. Because the shear force is calculated from the frictional pressure gradient, the correlation for frictional pressure gradient must be accurate. The correlation from Fuchs is used for frictional pressure gradient in Figure

4.5-1. The HEDH correlation deviates most from the single-phase liquid HTC at x=0. This could be caused by the fact that it is a correlation developed for highly sheared flow, which might not be the case at very low vapor fractions.

4.6 Multicomponent condensation heat transfer

4.6.1 Introduction

In multicomponent condensation the temperature at which the condensation occurs is gliding. The less volatile components will condense more readily than the more volatile components making the liquid and vapor equilibrium compositions vary as condensation takes place. As opposed to condensation of pure component sensible heat effects will also be present. In this section the most commonly used method for predicting two-phase HTC for multicomponent mixtures is presented.

4.6.2 Silver's method

The method is based on calculating an effective condensing side HTC that includes the resistance in the liquid film and the resistance in the vapor phase. The effective HTC is defined as [**12**]:

$$\alpha_{eff} = (\frac{1}{\alpha_l} + \frac{Z_g}{\alpha_g})^{-1}$$

Equation 4.6-1

where α_l is calculated from pure component correlation (sec. 4.5), and α_g is calculated from a single-phase correlation (sec. 4.4) with Reynolds number based on v_g (Equation A 19) and the tube diameter. The parameter Z_g is the ratio between sensible heat flux and total heat flux and is defined as:

$$Z_g = xcp_g \frac{dT}{dh}$$

Equation 4.6-2

The temperature in the gas core is assumed to follow the equilibrium condensing temperature of the mixture. Here the film thickness has been ignored so that the heat transfer area for the vapor against the liquid is assumed equal to the heat transfer area between the liquid and the wall. At low vapor fractions the heat transfer area between the gas and the liquid can be much smaller than between the liquid and the wall. If this is the case the gas-phase HTC should be multiplied with the ratio between the heat transfer areas.

Two important assumptions has been made here [**12**]:

1. Mass transfer effects is neglected
2. Any two-phase enhancement mechanisms have been neglected.

Correction for two-phase enhancement mechanisms is dealt with in the following section. Neeraas [**15**] found that mass transfer effects are small and can be neglected.

4.6.3 Modifications to Silver's method

Price and Bell [**17**] suggested a correction factor for interfacial surface roughness. The correction factor is multiplied with the gas-phase HTC.

$$C_f = \left[\frac{(\frac{dp}{dz})_{tp}^{fric}}{(\frac{dp}{dz})_{gs}^{fric}} \right]^{0.445}$$

Equation 4.6-3

The new gas-phase HTC is

$$\alpha_g^{cf} = C_f \alpha_g$$

Equation 4.6-4

Thome et al[**18**] suggests the same interfacial roughness correction factor for the gas phase HTC as the liquid phase HTC, namely fi defined by Equation A 18. The new gas phase HTC with the interfacial roughness correction factor is then

$$\alpha_g^{f_i} = f_i \alpha_g$$

Equation 4.6-5

The method by Thome et al was tested against measured HTCs for different refrigerant mixtures. The mixtures are different compositions of R125/236ea (98 points), R22/124 (77 points) and R290/600 (propane/butane, 659 points), and the ternary refrigerant R407C (38 points), which is a blend of R32, R125 and R124a (23,25,52 % by mass). Mass fluxes in the range 100-755 kg/m^{2}s and pressures up to 17 bar. Vapor fractions from 0.1 to 0.9.

Figure 4.6-1 shows f_i and C_f as a function of vapor fraction for the fluid and flow situation described in appendix C.

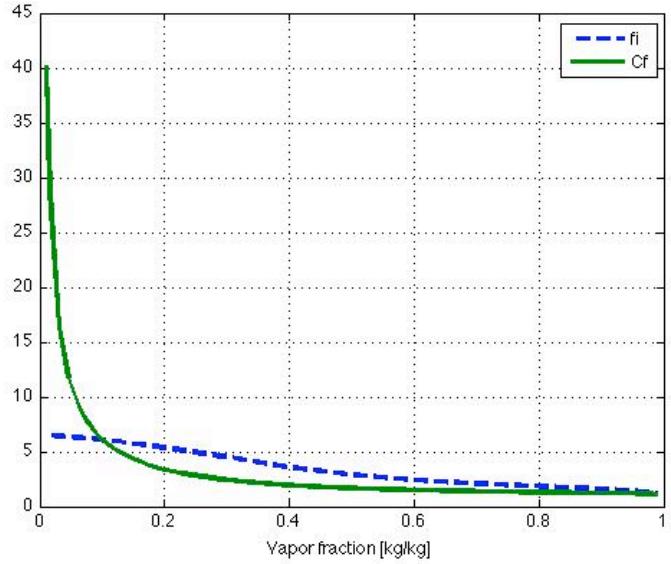

Figure 4.6-1 Surface roughness correction factors

A correlation from Fuchs[**19**] has been used to determine Cf. Cf becomes very large as the vapor fraction approaches zero, because the single phase gas pressure drop approaches zero as the vapor fraction approaches zero. At low vapor fractions most of the resistance against heat transfer is in the liquid so the fact that Cf becomes very large does not affect the effective two-phase HTC very much.

4.7 Comparison of HTC correlations in multicomponent condensation

Figure 4.7-1 shows effective HTCs as a function of vapor fraction for the flow situation and fluid described in appendix C. Since the same correlation is used for gas-phase HTC for all the effective mixture HTCs, the only additional deviation between the correlations compared to Figure 4.5-1 is the gas-phase enhancement factor. The enhancement factor from Price and Bell, C_f, is used on the gas phase HTC for the HEDH and modified Boyko and Kruzhilin correlation, while f_i is used on the Thome correlation as specified in the description of the model.

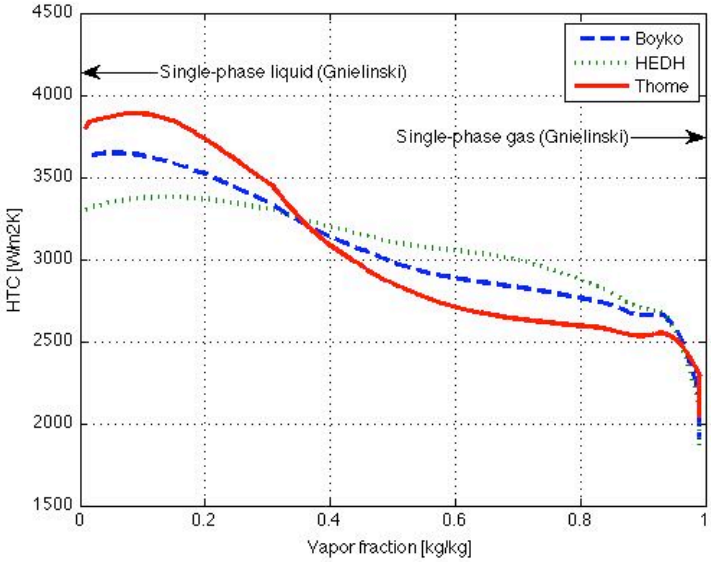

Figure 4.7-1 Effective mixture HTC comparison

The mixture HTC drops significantly at the transition from single-phase gas to two-phase. In contrast to condensation of pure components, where the HTC takes a sudden jump at the x=1 (Figure 4.5-1). This is because most of the resistance is in the gas-phase at high vapor fractions. The drop is caused by that the liquid that is formed smoothes out the tube walls, so the tube walls seem smooth from the gas-side. In single-phase gas flow the tube roughness tears up the laminar sub layer where most of the resistance against heat transfer is. In addition the interfacial roughness correction factors are 1 at the transition, because the waves that enhance heat transfer at the interface are proportional to the film thickness and the film thickness is low at high vapor fractions.

The model by Thome et al [**18**] predicted 75% of the HTCs measured from the R125/236ea and R407C mixtures to within 10%, but only predicts 50% of the measured HTCs (736 points) from the hydrocarbon mixtures to within 10%. This implies that this model does not predict accurate HTCs for hydrocarbons.

Neeraas [**15**] found that the modified Boyko and Kruzhilin method with C_f for interfacial enhancement gave good agreement with his experiments with methane/propane and ethane/propane mixtures. Mass fluxes in the experiments were in the range 150-400 kg/m^{2}s, vapor fractions between

0.08 and 0.98, and pressures between 16 and 40 bar. All measured HTCs were within 10%.

Another thing worth mentioning is that the deviation that the correlation from Thome showed without the mixture effects is suppressed by the fact that it is the gas phase HTC that is governing in that mass fraction interval. Though it is still lower than the other two correlations at mass fractions from 0.5 and up to 0.9.

4.8 Tube wall roughness effects in two-phase flow

How to handle the effect of tube wall roughness in two-phase flow is not described in the literature. The tube wall roughness will act on the liquid film, and tear up the thermal boundary layer in the liquid film. Intuitively, the same effects as in single-phase flow in tubes with rough walls should be encountered by the liquid film in annular flow. A two-phase friction factor is hard to define so the following tube-wall-roughness correction factor is proposed by the author:

$$\frac{\alpha_{film}}{\alpha_{film,smooth}} = \left(\frac{\left(\frac{dp}{dz}\right)_{fric}}{\left(\frac{dp}{dz}\right)_{fric,smooth}} \right)^{n}$$

Equation 4.8-1

where $n=0.68Pr_l^{0.275}$. This is based on Equation 4.4-6.

Figure 4.8-1 shows the correction factor as a function of vapor fraction for the fluid and flow situation in appendix C.

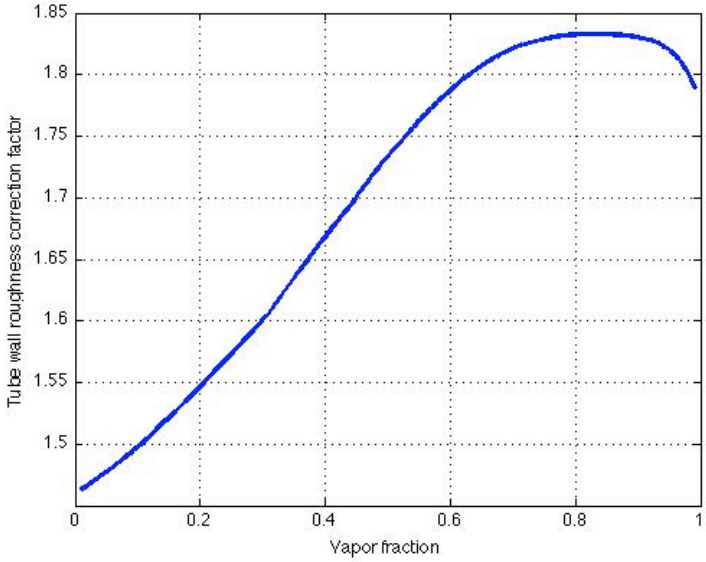

Figure 4.8-1 Tube wall roughness correction factor

The correlation from Fuchs is used for determining frictional pressure drop. It seems logic that the tube wall roughness has most impact when the liquid film is thin, because the thermal boundary layer is thicker compared to the liquid film thickness at high vapor fractions, than at lower vapor fractions.

Figure 4.8-2 shows the HTCs with the proposed correction factor. All of the correlations predict much higher HTCs than the single-phase liquid HTC at vapor fraction equal to zero. This implies that the proposed correction factor is not suited for two-phase flow.

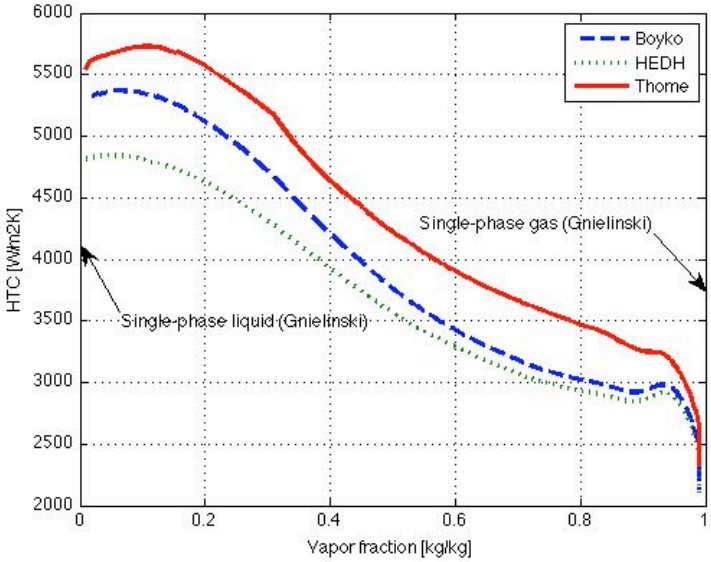

Figure 4.8-2 Two-phase HTC with wall roughness correction factor

It must be pointed out that Equation 4.8-1 has not been tested against any data from experiments and is solemnly a proposition by the author.

In the correlation by Boyko and Kruzhilin the effect of tube wall roughness is included in the liquid only HTC, while in the HEDH correlation the effects is indirectly included in the interfacial shear force which is calculated from the frictional pressure gradient.

Figure 4.8-3 shows a comparison for the same flow situation as described in appendix C, but with a lower tube wall roughness (0.002e-3 m). The correlation from Thome is unchanged while the two other decreases. This suggests that the modified Boyko and Kruzhilin or the HEDH correlation should be used for tubes with rough walls.

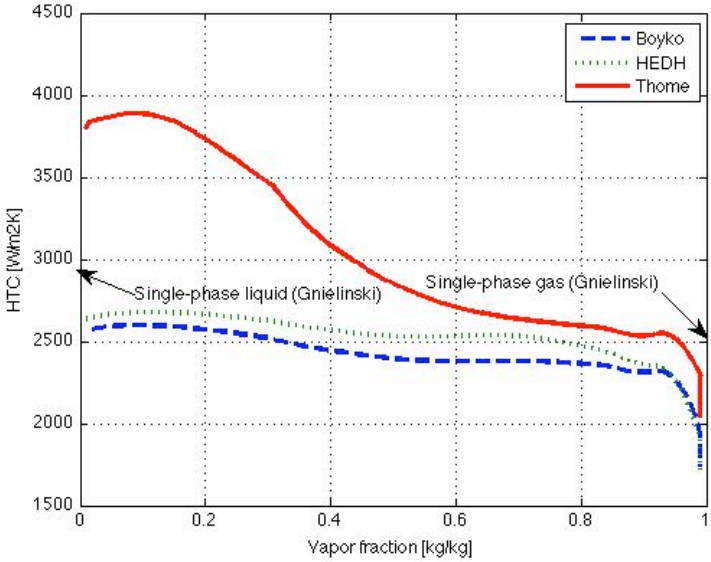

Figure 4.8-3 Comparison of HTC models with low wall roughness

Based on the discussion in the previous sections the modified Boyko and Kruzhilin correlation for liquid HTC and C_f as interfacial enhancement factor on gas-phase HTC seems most promising for HTC in condensation of mixtures.

4.9 Two-phase pressure drop

4.9.1 Static and momentum pressure drop

As mentioned previously pressure drop consists of three components: frictional pressure drop, momentum or acceleration pressure drop and pressure drop due to change in static height, expressed as

$$dp_{tot} = dp_{static} + dp_{momentum} + dp_{frictional}$$

Equation 4.9-1

Determining momentum and static pressure drop is a question of determining void fraction. Static pressure drop is defined as

$$dp_{static} = \rho_{tp} g dz$$

Equation 4.9-2

Where dz is the elevation change and the two-phase density is defined as

$$\rho_{tp} = \varepsilon \rho_g + (1-\varepsilon)\rho_l$$

Equation 4.9-3

Static pressure drop is zero for horizontal tubes. Momentum pressure drop is a function of condensation effects and is expressed as the difference between inlet and outlet conditions and can be calculated as:

$$dp_{acc} = -G^2 \left[\left(\frac{x^2}{\varepsilon \rho_g} + \frac{(1-x)^2}{(1-\varepsilon)\rho_l} \right)_{out} - \left(\frac{x^2}{\varepsilon \rho_g} + \frac{(1-x)^2}{(1-\varepsilon)\rho_l} \right)_{in} \right]$$

Equation 4.9-4

4.9.2 Frictional pressure drop

Frictional pressure drop is defined as [**20**]

$$-\frac{dp_{fric}}{dz} = \frac{\tau_w P}{A}$$

Equation 4.9-5

where τ_w is the shear stress at the tube wall, and P is the wetted perimeter (tube circumference for flow inside tubes).

There exist many empirical correlations for frictional pressure drop in two-phase flow. Four renowned correlations have been compared in this study:

- Lockhart and Martinelli[**21**]
- Chisholm[**22**]
- Friedel[**23**]
- Fuchs [**19**]

Description of the correlations can be found in Appendix B. The Lockhart and Martinelli correlation is historically the most widely used correlation, but it does not account for mass flux effects. Therefore more modern correlations such as Friedel's or Chisholm's correlations should be employed when possible [**20**]. The correlation by Fuchs is developed at the Norwegian Institute of Technology (now NTNU), department of refrigeration engineering (now department of energy and process engineering). The correlation has shown good agreement with various experiments at the institute [**15**], and is therefore interesting.

4.9.2.1 Comparison between the two-phase frictional pressure drop correlations

Figure 4.9-1 shows the predictions of pressure drop calculated from the different correlations for the fluid and flow situation described in appendix C.

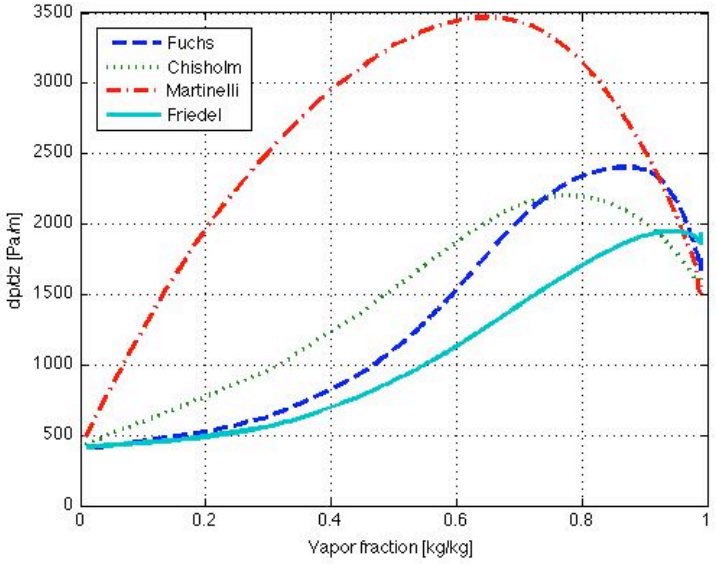

Figure 4.9-1 Frictional pressure drop

The Lockhart and Martinelli correlation predicts higher pressure-drop than all the other correlations, while the other three are fairly similar. Handbook of multiphase systems [**20**] gives these recommendations to when the different correlations should be used:

$\frac{\mu_l}{\mu_g} < 1000$	Friedel's correlation should be used
$\frac{\mu_l}{\mu_g} > 1000$ and G>100	Chisholm's correlations should be used
$\frac{\mu_l}{\mu_g} > 1000$ and G<100	Lockhart and Martinelli's correlation should be used

Table 4.9-1 Recommendations to frictional pressure drop correlations

The correlation by Friedel is developed from a database of 25000 data points and is for vertical upward and horizontal flow. The standard deviation was about 40-50% for two-component flows [**20**]. Chisholm's correlation is derived from the Lockhart-Martinelli approach, but with additional parameters to account for fluid properties and mass flux.

The correlation from Fuchs was not mentioned in the Handbook of multiphase systems, but Neeraas [**15**] found it to over-predict the pressure-drop for his experiments. He also found that the deviation increased with

pressure. Based on this he proposed a correction factor as a function of the liquid-gas density ratio and the vapor fraction. The correction is found in appendix B.

The corrected Fuchs correlation was within 10% of his experiments at vapor fractions between 0.3 and 0.9. At vapor fractions above 0.9 he explained the deviation with the desire to hit the single-phase value at x=1. At vapor fractions below 0.3 he stated that the deviation could be caused by a change in flow pattern.

Figure 4.9-2 shows a comparison between the corrected Fuchs and the original Fuchs.

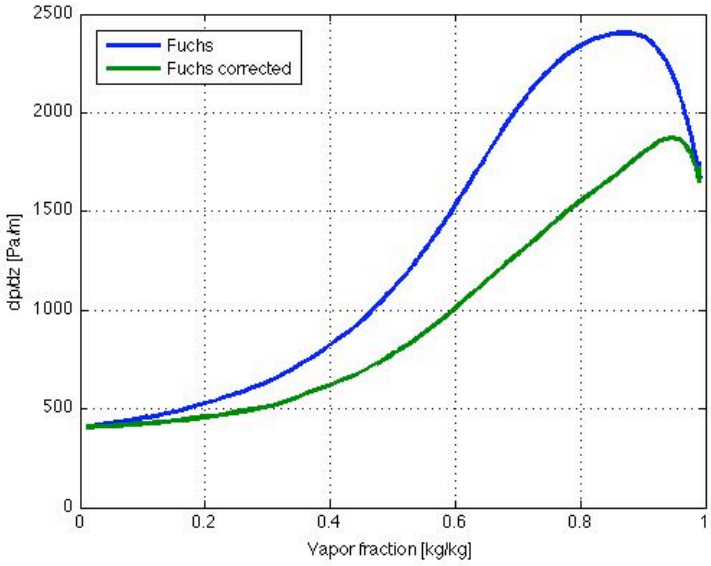

Figure 4.9-2 Comparison of original and corrected Fuchs

The corrected Fuchs predicts generally lower values than the original Fuchs, which corresponds to Neeraas' experiments. For this specific case the viscosity ratio is between 5 and 10. The handbook of multiphase systems suggests the Friedel correlation for viscosity ratio below 1000. Figure 4.9-3 shows a comparison between Friedel and the corrected Fuchs. The resemblance is striking.

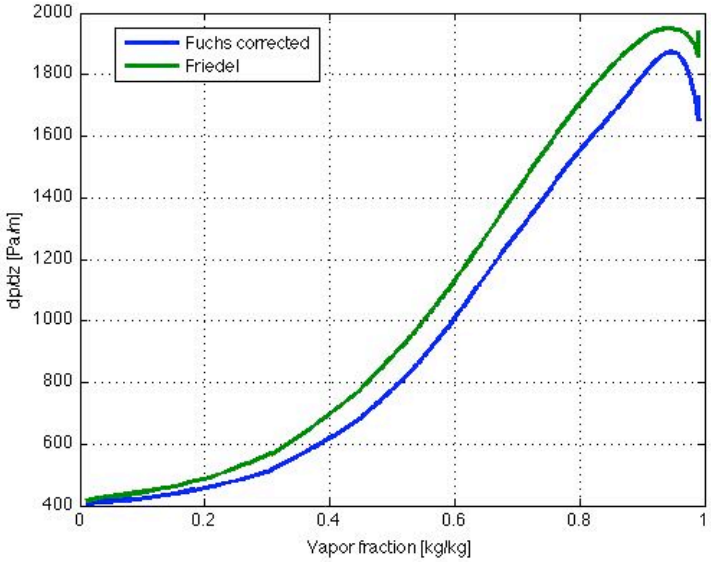

Figure 4.9-3 Fuchs corrected and Friedel correlation

Since Neeraas' experiments were carried out with mixtures of hydrocarbons and he found good agreement with the corrected Fuchs correlation, this correlation is used in the model.

In the HEDH correlation for liquid HTC during condensation the interfacial shear force is calculated from the frictional pressure gradient. In Figure 4.7-1 the original Fuchs correlation is used. In addition, the frictional pressure gradient is used in the two-phase enhancement factor for the gas-phase HTC in two-phase flow (Equation 4.6-3). Figure 4.9-4 shows the same comparison, but with the corrected Fuchs for calculation of the interfacial shear force and the gas-phase enhancement factor (C_f).

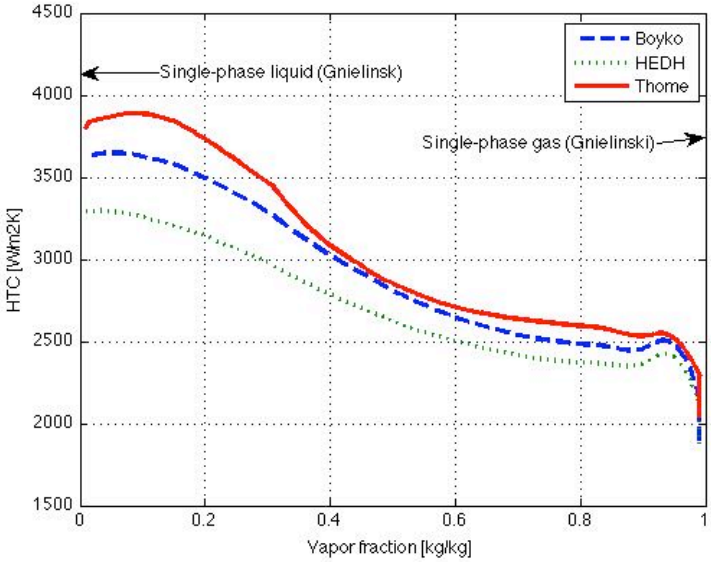

Figure 4.9-4 HTC with corrected Fuchs

The HEDH correlation generally becomes a little lower because the lower predicted interfacial shear force by the corrected Fuchs.

4.10 Natural convection around immersed bodies

If tubes are immersed in a stagnant fluid and there is a temperature difference between the tube wall and the bulk fluid, a density difference will occur and this will induce fluid motion. The fluid motion increases heat transfer compared to pure conduction. This heat transfer mechanism is known as natural or free convection. In this section methods for calculating the HTC for natural convection around immersed tubes will be presented. The whole section is based on HEDH[**12**] and Cengel[**9**].

For flow in channels the Reynolds number is a measure of inertia forces to viscous forces, and is an indication of if the flow is turbulent or not. The corresponding dimensionless number for natural convection is the Grashof number. The Grashof number represents the buoyancy forces to viscous forces, and is defined as:

$$Gr = \frac{g\beta(T_s - T_\infty)l_c^3}{\upsilon^2}$$

Equation 4.10-1

Where β is volume of expansion, T_∞ is the bulk fluid temperature, l_c is the characteristic length, which is the tube diameter for a horizontal tube and the axial position for a vertical tube, T_s is the surface temperature and υ is

the kinematic viscosity. For vertical tubes the characteristic length varies with the distance from the tubes leading edge. This is because the boundary layer increases with position. The critical Grashof number for vertical plates is 10^9, that is, the boundary layer becomes turbulent when the Grashof number exceeds 10^9. In natural convection it is usual to specify the range of where a correlation is valid based on the Rayleigh number, which is the product of the Grashof number and the Prandtl number.

$$Ra = Gr\,\mathrm{Pr}$$

Equation 4.10-2

In natural convection around horizontal cylinders the thickness of the boundary layer around the periphery of the cylinder will differ (see Figure 4.10-1), but correlations for the average Nusselt number around the periphery have been proposed. HEDH proposes the following correlation, which is valid for both laminar and turbulent boundary layer:

$$\overline{Nu_f} = \frac{0.518\,Ra^{1/4}}{\left[1+(0.559/\mathrm{Pr})^{9/16}\right]^{4/9}} \times \left(1+\frac{3.47\times10^{-1}\,Ra}{\left[1+(0.559/\mathrm{Pr})^{9/16}\right]^{16/9}}\right)^{1/12}$$

Equation 4.10-3

A correction factor for the curved thickness of the boundary layer is also proposed:

$$\overline{Nu} = \frac{2}{\ln(1+2/\overline{Nu_f})}$$

Equation 4.10-4

The fluid properties should be evaluated at the film temperature, defined as the arithmetic mean between the wall temperature and the bulk fluid temperature.

$$T_{film} = \frac{T_s + T_\infty}{2}$$

Equation 4.10-5

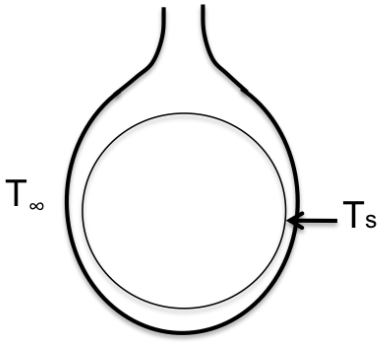

Figure 4.10-1 Curved boundary layer around tube

For vertical plates (assumed valid for vertical tubes) HEDH[**12**] proposes the following relationship for the laminar regime with constant wall temperature, Rayleigh numbers (based on the axial position) between 10^4 and 10^9

$$Nu = 0.503\left[Ra_x \left(1 + \left(\frac{0.492}{\Pr} \right)^{9/16} \right)^{-16/9} \right]^{1/4}$$

Equation 4.10-6

For Rayleigh numbers greater than 10^{12}, turbulent boundary layer, the following expression is suggested by HEDH

$$Nu = 0.15\left[Ra_x \left(1 + \left(\frac{0.492}{\Pr} \right)^{9/16} \right)^{-16/9} \right]^{1/3}$$

Equation 4.10-7

The subscript x denotes that it is Rayleigh number based on the distance along the tube. The transition from laminar to turbulent seems hard to decide. But based on the mentioned ranges for Rayleigh numbers in the laminar and turbulent regime, the transition starts at 10^9. Based on this Equation 4.10-6 and Equation 4.10-7 can be combined into the following expressions that yields both for the transition and the turbulent regime[**12**]. That is, Rayleigh numbers greater than 10^9.

$$Nu = 89.4\Pr^{1/4}\left(\left(1 + \left(\frac{0.492}{\Pr} \right)^{9/16} \right)^{-16/9} \right)^{1/4} + 0.15\left(Ra_x^{1/3} - 1000\Pr^{1/3} \right)\left(\left(1 + \left(\frac{0.492}{\Pr} \right)^{9/16} \right)^{-16/9} \right)^{1/3}$$

Equation 4.10-8

4.11 External forced convection

External forced convection is basically governed by the same mechanisms as internal convection heat transfer described in sec 4.4, but flow around bodies introduce additional effects. In this section it is important to differentiate between flow across tubes, know as cross flow, and flow along tubes, which can be looked upon as flow over a flat plate.

4.11.1 Flow across tubes

Flow across tubes involve flow separation, that is, the boundary layer does not manage to follow the curvature of the tube and separates and forms a wake at the rear of the cylinder as illustrated in Figure 4.11-1.

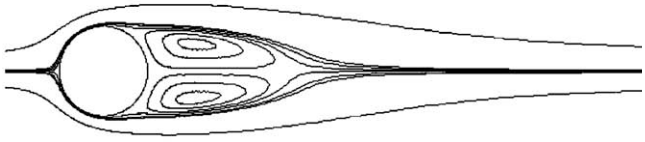

Figure 4.11-1 Boundary layer separation[24**]**

This fact makes it hard to handle analytically, but correlations have been formed that correlate the available data well. Cengel[**9**] suggests the following correlation from Churchill and Bernstein:

$$Nu = 0.3 + \frac{0.62\,\mathrm{Re}^{1/2}\,\mathrm{Pr}^{1/3}}{\left[1+(0.4/\mathrm{Pr})^{2/3}\right]^{1/4}}\left[1+\left(\frac{\mathrm{Re}}{282000}\right)^{5/8}\right]^{4/5}$$

Equation 4.11-1

The Nusselt number is the same as for internal flow and defined by Equation 4.4-2 with the tube diameter as the characteristic length. The characteristic length in the Reynolds number is also the tube diameter, and the properties should be evaluated at the film temperature.

4.11.2 Flow over a horizontal plate (tube)

Flow over flat plates involves a laminar boundary layer at start of the plate, transition to turbulent, and fully developed turbulent boundary layer. The HTC differs in the different boundary layer regimes. The transition to turbulent boundary layer depends on many variables, but the Reynolds number characterizes the boundary layer best. The characteristic length in the Reynolds number and the Nusselt numbers is the distance x along the plate from the leading edge,

$$\mathrm{Re} = \frac{\rho V x}{\mu}$$

Equation 4.11-2

Local Nusselt numbers for laminar and turbulent flow are respectively [**9**]

$$Nu = 0.332\,\mathrm{Re}^{0.5}\,\mathrm{Pr}^{1/3}$$

Equation 4.11-3

$$Nu = 0.0296\,\mathrm{Re}^{0.8}\,\mathrm{Pr}^{1/3}$$

Equation 4.11-4

The transition regime starts at Reynolds number of 10^5 and becomes fully turbulent at about $3*10^6$ [**9**]. Again, the properties should be evaluated at the film temperature.

4.12 Combined forced and natural convection

External forced convection is always accompanied with natural convection, because there will always be a density difference in a fluid when there is a temperature difference. Because HTC tends to increase when fluid velocity increases we normally ignore the natural convection affect when forced convection is present. Cengel[**9**] states that the parameter Gr/Re^2 represents the importance of natural convection relative to forced convection. When $Gr/Re^2 < 0.1$ natural convection is negligible, when $Gr/Re^2 > 10$ forced convection is negligible. In the range between neither is negligible and both affects must be taken into account.

The buoyant motion will have different direction depending on if the surface is hot or cold, in this study the surface will be hotter than the surrounding fluid so the buoyant motion will be upwards. If the external flow is opposing to the buoyant motion the forced convection resists the natural convection, leading to a decrease in HTC, similarly it will lead to an increase in HTC if the external flow is in the same direction as the buoyant motion, known as assisting flow. In cross flow the buoyant motion is perpendicular to forced flow. The cross flow leads to enhanced mixing, and hence, increased heat transfer.

Both Cengel[**9**] and HEDH[**12**] proposes the following expression for HTC for combined natural and forced convection:

$$Nu_{combined} = (Nu^n_{forced} \pm Nu^n_{natural})^{1/n}$$

Equation 4.12-1

The minus sign for opposing flow and plus for assisting and cross flow. The exponent n varies based on geometry. For immersed bodies in cross flow or assisting flow HEDH suggest n equal to 4.

Figure 4.12-1 shows outer HTC in parallel flow over a horizontal tube as a function of seawater velocity for different temperature differences between the tube wall and the seawater.

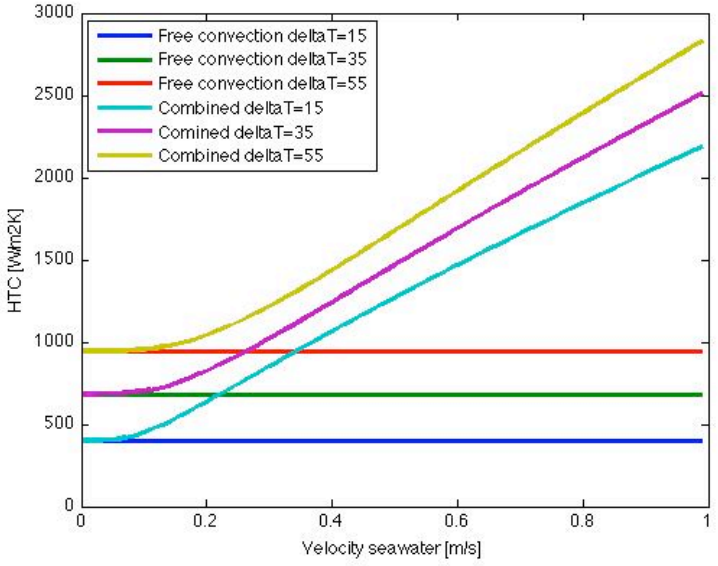

Figure 4.12-1 Outer HTC in parallel flow

The natural convection term increases with temperature difference, and has an influence on the combined HTC up to higher seawater velocities. But even at the highest temperature difference the forced convection term dominates the combined HTC at seawater velocities from 0.2 and upward.

Figure 4.12-2 shows the same as Figure 4.12-1, but for cross flow. Here, the forced convection term dominates the combined HTC even at very low seawater velocities.

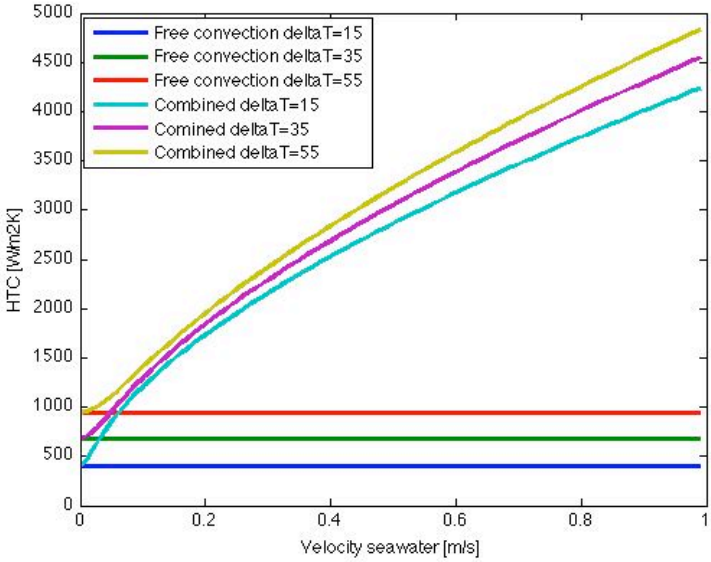

Figure 4.12-2 Outer HTC in cross flow

A conclusion that can be drawn from this is that knowledge of the direction of the seawater and the seawater velocity is crucial for estimating HTC on the outside of tubes. In a subsea heat exchanger with the surrounding water as coolant this information is very uncertain and may change continuously. In an active cooler where the coolant velocity is controlled, the outlet temperature can easier be controlled.

4.13 Seawater velocity's impact on overall HTC

If the heat transfer mechanism is solemnly natural convection on the outside of the tubes, the resistance against heat transfer will normally be on the outside of the tubes. The smallest HTC will be the limiting factor in the overall HTC, (see Equation 5.2-5). This means that when the resistance is on the outside, good prediction of the outer HTC is much more crucial than the inner HTC. But as the velocity increases the limiting HTC can change from the outside to the inside. If this is the case, then good prediction of inner HTC is crucial. In the condensation of mixtures different HTC models give different results, Therefore, choice of inner HTC correlation must be paid great attention if the velocity of the seawater is substantial.

5 Heat exchanger design theory

5.1 Introduction

There are numerous kinds of heat exchangers, but the theory in this chapter focuses on tube heat exchangers with various types of flow orientation on the outside of the tubes. The flow on the outside of the tubes can be counter-current, co-current, cross flow or stagnant.

This chapter is based on references [**9**], [**25**]

5.2 Overall heat transfer coefficient

In order to decide how much heat that is transferred from the fluid inside the tubes to the fluid on the outside of the tubes for a given temperature difference it is necessary to decide the overall heat transfer coefficient. The heat is transferred by convection from the bulk fluid to the tube wall, then by conduction through the tube wall, and finally by convection from the tube wall to the bulk fluid on the outside of the tubes.

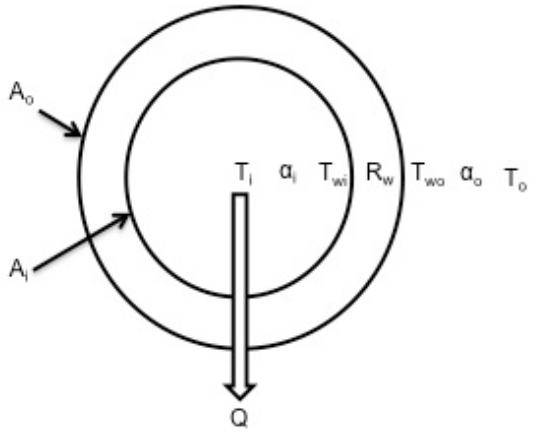

Figure 5.2-1 Heat transfer

Energy conservation gives that the heat transfer rate must be constant from inside the tube, to outside the tube. The rate of heat transfer for a segment of the tube is then

$$dQ = dA_i\alpha_i(T_i - T_{wi}) = \frac{(T_{wi} - T_{wo})}{R_w} = dA_o\alpha_o(T_{wo} - T_o)$$

Equation 5.2-1

Eliminating the wall temperatures from Equation 5.2-1 gives the following expression

$$dQ = \frac{T_i - T_o}{\frac{1}{\alpha_i dA_i} + R_{wall} + \frac{1}{\alpha_o dA_o}}$$

Equation 5.2-2

where

$$R_{wall} = \frac{\ln \frac{D_o}{D_i}}{2\pi\lambda_w dL}$$

Equation 5.2-3

It is desirable to express the rate of heat transfer from the temperature difference, an overall HTC, and a heat transfer area. But since the heat transfer area is different on the outside of the tube and on the inside of the tube it is necessary to specify if the overall HTC is based on inner or outer heat transfer area. The final expressions if the overall HTC based on the outer area is:

$$dQ = dA_o U_o (T_i - T_o)$$

Equation 5.2-4

where

$$U_o = \left(\frac{dA_o}{dA_i \alpha_i} + R_{wall} dA_o + \frac{1}{\alpha_o} \right)^{-1} = \left(\frac{D_o}{D_i \alpha_i} + \frac{D_o \ln \frac{D_o}{D_i}}{2\lambda_w} + \frac{1}{\alpha_o} \right)^{-1}$$

Equation 5.2-5

5.3 Calculation of temperature profile tube side

The heat transferred from the fluid inside the tubes is:

$$dQ = -\dot{m}\, dh_i$$

Equation 5.3-1

For heat transfer without condensation this expression simplifies to

$$dQ = -\dot{m} c_p dT_i$$

Equation 5.3-2

Combining Equation 5.2-4 and Equation 5.3-2 gives the following differential equation for the temperature inside the tubes in single-phase flow:

$$\frac{dT_i}{dA_o} = -\frac{U_o(T_i - T_o)}{\dot{m} c_p}$$

Equation 5.3-3

The overall HTC and the heat capacity may vary along the length of the tube, and must be calculated for each segment. The temperature of the fluid on the outside may not be known, depending on configuration. This will be discussed in section 5.4.

If condensation occurs the rate of heat transferred in each segment is calculated from Equation 5.2-4, the new enthalpy of the two-phase mixture is calculated by subtracting the heat transferred in the segment from the enthalpy in the previous segment. The new temperature and properties is then obtained by interpolating in tables at the new enthalpy.

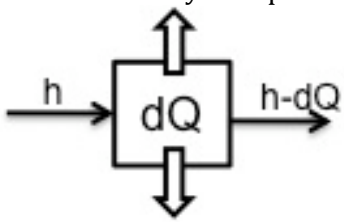

Figure 5.3-1 Heat transfer in segment

5.4 Water side configurations and heat transfer

The fluid on the outside of the tubes will from now on be referred to as water, and the outside will be referred to as waterside. In this study seawater will be the coolant on the outside of the tubes, so it is convenient to use these names. The equations for temperature profiles on the seawater in the following section will only be necessary to solve in a closed arrangement. In an open arrangement the temperature of the seawater will be constant.

5.4.1 Natural convection

In natural convection the water temperature is assumed constant and equal to seawater temperature. The outer HTC is explicitly a function of the outside wall temperature, and implicitly through the properties, which should be evaluated at the film temperature, as mentioned.

5.4.2 Co-current flow

In a co-current arrangement the external flow is parallel to the internal flow as illustrated in Figure 5.4-1.

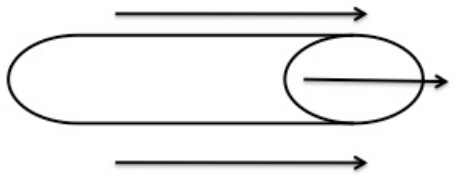

Figure 5.4-1 Co-current flow

The rate of heat transferred to the water is calculated from Equation 5.2-4, and the temperature profile of the water is calculated by integrating the following equation from tube inlet to tube outlet:

$$\frac{dT_o}{dA_o} = \frac{U_o(T_i - T_o)}{\dot{m}_o cp_o}$$

Equation 5.4-1

5.4.3 Countercurrent

In a countercurrent configuration the external flow is flowing in the opposite direction of the internal flow, illustrated below.

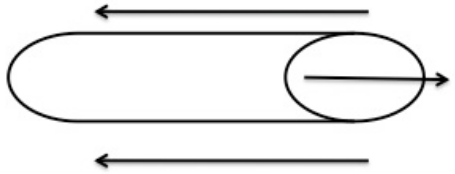

Figure 5.4-2 Countercurrent flow

In this case the external and internal temperatures are not known at the same location. This leads to that the water temperature at the inlet of the tube has to be guessed. And the following differential equation integrated from tube inlet to tube outlet.

$$\frac{dT_o}{dA_o} = -\frac{U_o(T_i - T_o)}{\dot{m}_o cp_o}$$

Equation 5.4-2

If the calculated water temperature at the tube outlet is equal to the actual water temperature the problem is solved, if not, a new guess of water temperature at the tube inlet has to be made. This must be repeated until the actual water temperature is reached at the tube outlet.

5.4.4 Cross flow

In a cross flow configuration the flow is perpendicular to the tube axis. Cross flow can be further classified into unmixed or mixed flow. The cross flow is said to be unmixed if the flow is prohibited from moving in the transverse direction with physical separation, or if it is assumed not to move in the transverse direction. Figure 5.4-3 illustrates this from a birds view.

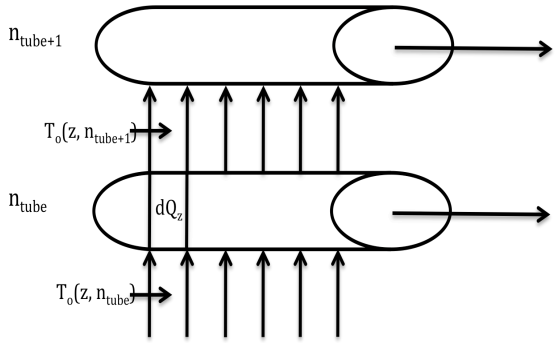

Figure 5.4-3 Cross flow unmixed

The temperature of the water will vary along the length of the tube, and can be calculated as:

$$T_o(z,ntube+1) = T_o(z,ntube) + \frac{dQ_z}{\dot{m}_o\, cp_o}$$

Equation 5.4-3

Where ntube denotes the tube number and dQ_z is the heat transferred at a distance z along the tube. dQ_z is calculated from Equation 5.2-4.

In mixed cross flow the fluid is free to move in the transverse direction, and the temperature does not vary along the axis of the tube because of this mixing.

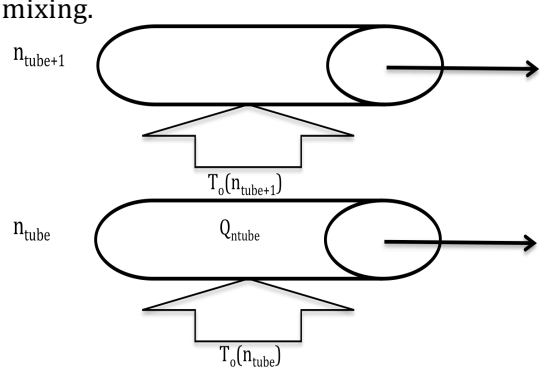

Figure 5.4-4 Cross flow mixed

The water temperature is calculated as:

$$T_o(ntube+1) = T_o(ntube) + \frac{Q_{ntube}}{\dot{m}_o \, cp_o}$$

Equation 5.4-4

Where Q_{ntube} is the total heat transferred from the "previous" tube.

5.5 Tube side maldistribution

Varying external conditions can induce maldistribution. The pressure drop through each tube must be equal for the flow to be stable. If the water temperature varies outside the different tubes the heat transfer will be affected and this will affect the pressure drop as well. Nature will distribute the total mass flow into the tubes so that the pressure drop in each tube becomes equal. This leads to different outlet conditions in each tube.

In two-phase flow there can also be maldistribution at the inlet. If the liquid is distributed unequally through the header nature distributes the gas in such a way that equal pressure drop is experienced in each tube. This is not included in the model because this would lead to different equilibrium condensation curves in each tube. In order to solve this an equation of state must be implemented, and that is not under the scope of this study.

5.6 Fouling in heat exchangers

Fouling is a coating that forms in heat exchangers over time. The formation of fouling is an additional resistance against heat transfer. In a subsea heat exchanger fouling on the outside of tubes is likely to occur. Extra heat transfer area is necessary in order to reach the specified outlet temperature. Since it is difficult to add extra heat transfer area after a heat exchanger has been installed, future fouling should be included in the design process. The fouling resistance is included in the overall HTC as follows:

$$U_o = \left(\frac{D_o}{D_i \alpha_i} + \frac{D_o \ln \frac{D_o}{D_i}}{2\lambda_w} + R_{f,o} + \frac{1}{\alpha_o} \right)^{-1}$$

Equation 5.6-1

Where $R_{f,o}$ is the fouling resistance on the outside of tubes. There are several types of fouling, and the principal processes that cause the fouling

classify them. The types of fouling that is most likely to form in a subsea heat exchanger are deposition fouling, corrosion fouling, particle fouling and biological fouling. These are described in [**25**]. The coating of the tubes will also affect the heat transfer and this resistance can be included in the fouling resistance.

6 Modeling

6.1 Introduction

This chapter deals with how the calculation model is built. The calculation model is implemented in the commercial software MATLAB (Matrix Laboratory). The most important parts of the programming, and special considerations is mentioned under this chapter. An overview and description of the routines and the complete m-files can be found in appendix D.

The model is based on tubes in parallel with various configuration of the seawater flow. Both horizontal are vertical tubes are implemented. The tubes are assumed straight (no bends).

6.2 Discretization and numerical integration

In order to use numerical integration the continuous tube must be divided into discrete segments where the fluid temperature, pressure and fluid properties are constant. The nodes can either be placed in the middle of the segment or at the end of each segment. Here it is chosen to place them at the end of each segment, as shown in Figure 6.2-1.

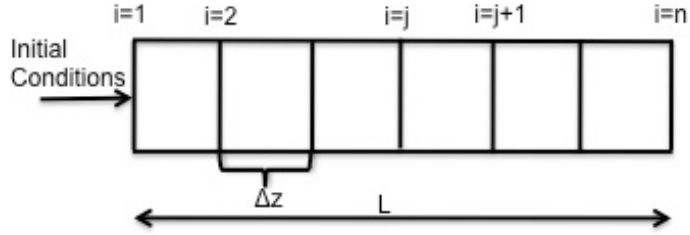

Figure 6.2-1 Discretization and node placement

The differential equations Equation 5.3-3, Equation 5.4-1 and Equation 5.4-2 must be discretized in order to solve them numerically. Since the tube diameter is constant the left hand side of the mentioned equations simplifies to constant*dT/dz, where z is the distance along the tube. By the use a forward difference this gradient can be discretized as follows [**26**]

$$\frac{dT_i}{dz} = \frac{T_{i+1} - T_i}{\Delta z}$$

Equation 6.2-1

By solving the equation with respect to T_{i+1} the forward Euler scheme[**26**] is obtained

$$T_{i+1} = T_i + \Delta z \left(\frac{dT}{dz} \right)_i$$

Equation 6.2-2

Euler's method is a first order method. This means that the global error is of order Δz. This requires small values of Δz in order to achieve accurate results.

6.3 Temperature profiles

Inserting for dT_i/dz from Equation 5.3-3 gives the following expression for the tube side temperature in single-phase flow.

$$T_{i+1} = T_i - \Delta z \frac{U_o \left(T_i - T_{o,i} \right) \pi D_o}{\dot{m} c_p}$$

Equation 6.3-1

T_i denotes the bulk temperature inside the tubes in ith node, and $T_{o,i}$ denotes the bulk temperature on the outside of a tube at the ith node. The overall HTC and specific heat capacity should (as implied by Equation 6.2-2) be evaluated at the conditions of the ith node. Similarly the expressions for water temperature in co-current and countercurrent flow in a closed arrangement are respectively

$$T_{o,i+1} = T_{o,i} - \Delta z \frac{U_o (T_i - T_o) \pi D_o}{\dot{m}_o \, cp_o}$$

Equation 6.3-2

$$T_{o,i+1} = T_{o,i} + \Delta z \frac{U_o (T_i - T_o) \pi D_o}{\dot{m}_o \, cp_o}$$

Equation 6.3-3

In the case of an open heat exchanger the mass flow of the water will be infinite and the water temperature will be constant.

In condensing flow an explicit relation can't be formed without use of an equation of state. This is not under the scope of this study. Instead the temperature is assumed to follow the equilibrium condensing temperature slope for the mixture. The temperature in the "next" node is obtained by calculating the heat transferred in the ith segment as:

$$\Delta Q_i = U_o \pi D_o (T_i - T_{o,i}) \Delta z$$

Equation 6.3-4

The new enthalpy is

$$h_{i+1} = h_i - \Delta Q_i$$

Equation 6.3-5

Then the temperature is obtained by interpolating in a table with the new enthalpy.

The outside wall temperature, T_W, of the tube is necessary in order to calculate the properties of the water. As mentioned earlier, water properties should be evaluated at the film temperature, $0.5(T_W+T_0)$. From a heat balance the wall temperature can be calculated as:

$$T_{w,i+1} = T_i - \frac{U_o}{U_{iw}}\left(T_i - T_{o,i}\right)$$

Equation 6.3-6

Where U_{iw} is the total HTC from the fluid inside the tube to the tube outside wall

$$U_{iw} = \left(\frac{D_o}{D_i \alpha_i} + \frac{D_o}{2\lambda_w} \ln \frac{D_o}{D_i} \right)^{-1}$$

Equation 6.3-7

All the mentioned temperature profiles in this section may vary from tube to tube if the water flow is in cross flow with the tubes so that the water temperature differs from tube to tube. In that case the temperature terms should have an additional index. For example Equation 6.3-1 could be written as follows

$$T^{j}_{i+1} = T^{j}_{i} - \Delta z \frac{U_o \left(T^{j}_{i} - T^{j}_{o,i}\right) \pi D_o}{\dot{m} c_p}$$

Equation 6.3-8

But in order to keep the expressions as plain as possible this index is not included in the expressions. The same goes for the pressure profiles in the following chapter.

6.4 Pressure profiles

The pressure profile in a tube is calculated in the same manner as the temperature profiles.

$$P_{i+1} = P_i + \Delta z \left(\frac{dp}{dz} \right)_i$$

Equation 6.4-1

As mentioned earlier the pressure gradient is the sum of three contributions. For single-phase flow the frictional pressure gradient is calculated from Equation 4.3-2 with Equation 4.3-7 for the friction factor. The expressions for momentum and static pressure-drop must be discretized. For the static pressure drop in single-phase flow in vertical tubes the following expression is used

$$\left(\frac{dp}{dz}\right)_{static,i} = \frac{\rho_i + \rho_{i+1}}{2} g$$

Equation 6.4-2

Equation 4.9-4 discretized gives the momentum pressure-drop as:

$$\left(\frac{dp}{dz}\right)_{momentum,i} = -\frac{G^2}{\Delta z}\left[\left(\frac{x_{i+1}^2}{\varepsilon_{i+1}\rho_{g,i+1}} + \frac{(1-x_{i+1})^2}{(1-\varepsilon_{i+1})\rho_{l,i+1}}\right) - \left(\frac{x_i^2}{\varepsilon_i\rho_{g,i}} + \frac{(1-x_i)^2}{(1-\varepsilon_i)\rho_{l,i}}\right)\right]$$

Equation 6.4-3

It is possible to use the conditions at i+1 because the temperature is calculated before the pressure. Equation A 15-Equation A 17 is used for calculating the void fraction.

If the tubes are vertical the static pressure drop in two-phase flow is calculated by the following discretization

$$\left(\frac{dp}{dz}\right)_{static,i} = g\left[\left(\frac{\rho_{g,i+1} + \rho_{g,i}}{2}\right)\left(\frac{\varepsilon_{i+1} + \varepsilon_i}{2}\right) + \left(\frac{\rho_{l,i+1} + \rho_{l,i}}{2}\right)\left(1 - \frac{\varepsilon_{i+1} + \varepsilon_i}{2}\right)\right]$$

Equation 6.4-4

For the frictional pressure gradient in two-phase flow the corrected correlation by Fuchs is used. Introducing the discretized syntax and rearranging, the expression becomes

$$\left(\frac{dp}{dz}\right)_{frictional,i} = \psi(x_i)\left(\left(\left(\frac{dp}{dz}\right)_{fric,go,i} - \left(\frac{dp}{dz}\right)_{fric,lo,i}\right) + \left(\frac{dp}{dz}\right)_{fric,lo,i}\right) f\left(\frac{\rho_{l,i}}{\rho_{g,i}}, x_i\right)$$

Equation 6.4-5

The single-phase pressure gradients are calculated as described for single-phase flow, but with the respective Reynolds numbers.

Total pressure gradient is:

$$\left(\frac{dp}{dz}\right)_i = \left(\frac{dp}{dz}\right)_{momentum,i} - \left(\frac{dp}{dz}\right)_{static,i} - \left(\frac{dp}{dz}\right)_{frictional,i}$$

Equation 6.4-6

The momentum term is chosen positive because during cooling and condensation this term increases the pressure. This sign convention has been chosen in order to get all the quantities positive.

6.5 Evaluating fluid properties

An equation of state is not included in the calculation model. Therefore, the user must specify thermodynamic and physical properties. This is most conveniently done in a table in excel format or such. In order to extract the properties at a specific temperature, interpolation in the table must be carried out. MATLAB can read excel-files and extract the data in the tables. In order to generalize the program code the table should be in a specified form. The form is shown in Figure 6.5-1

Temperature
Pressure
Enth (kJ/kg)
Gas molfrac (mol%)
Gas massfrac (mass%)
Total density (kg/m3)
Gas density (kg/m3)
Liquid density (kg/m3)
Gas viscosity (cP)
Liquid viscosity (cP)
Gas CP (kj/kgK)
Liquid CP (kj/kgK)
Gas thermal conduc (mW/mC)
Liquid thermal conduc (mW/mC)
Oil/gas interfacial tension (mN/m)

Figure 6.5-1 Properties input table

When the table is read by MATLAB and the data is saved in variables in MATLAB the built-in function *interp1* can be used to interpolate in the table. The method of interpolation can be specified in the *interp1* function. Problems can occur at the transition from single phase to two-phase flow because there are no points to interpolate between. In order to avoid this problem a method that extrapolates if necessary is chosen. The method *spline* uses cubic spline interpolation, and extrapolates if necessary. This method is chosen in the program code.

6.6 Wall inlet temperature

At the inlet, the outside wall temperature is not known. The outer wall temperature is necessary in order to obtain the outer HTC. Since these are both unknown an iteration loop is necessary for deciding outer HTC and

outside wall temperature at the inlet. From a heat balance the following relation can be established at the tube inlet:

$$dA_o U_o (T_1 - T_{o,1}) = dA_o U_{iw} (T_1 - T_{wo,1})$$

Equation 6.6-1

U_o and U_{iw} are functions of the wall temperature. An iteration loop where T_{wo} is changed until Equation 6.6-1 is satisfied within a given tolerance is implemented in the function *twallstart.*

6.7 Pressure drop iteration

The temperature and pressure profiles are solved for each tube separately. A *for*-loop with a given step size (Δz) is used for integrating through each tube. This is done in a tube-by-tube manner. The "first" tube is integrated over the length of the tube first, then the second and so on. Since the seawater temperature may differ around each tube (in cross flow with a finite water mass flow rate) the pressure drop may also vary, as mentioned before. When the temperature and pressure profiles in each tube have been achieved the pressure drop in each tube is compared. The pressure drop in each tube is saved in a variable, and with help of the built-in MATLAB functions *max* and *min* the minimum and maximum pressure drop is found. The built-in MATLAB functions *max* and *min* also return in which tube the maximum and minimum pressure-drops are. If the difference between maximum and minimum pressure drop is greater than a give tolerance the total mass flow has to be redistributed until the difference in pressure drop is under the tolerance level. Figure 6.7-1 illustrates this iteration process.

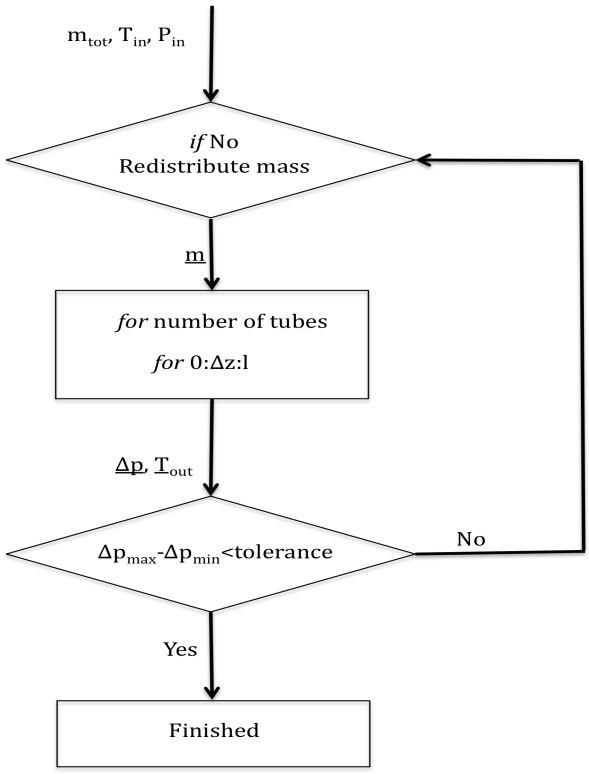

Figure 6.7-1 Iteration process in order to get equal pressure drop in each tube

The underlined symbols in Figure 6.7-1 are vectors.
The first guess is of course to distribute the total mass flow rate evenly through all the tubes. When redistributing the mass flow rate the total mass balance must be fulfilled. That is, if the mass flow rate is increased in one tube, it must be reduced by the same quantity in another tube. In order to get the program to run reasonably fast the redistribution should be done in a smart way. The following logic is used in the program code for deciding how to redistribute the mass:

$$\Delta p \sim lG^2$$

Equation 6.7-1

$$\frac{\Delta p_{\max} - \Delta p_{\min}}{2} \sim \Delta G^2 l$$

Equation 6.7-2

$$\Delta m = \frac{\left(\Delta p_{\max} - \Delta p_{\min}\right)^{1/2}}{2l} D_i^2$$

Equation 6.7-3

Δm is subtracted from the tube with the highest pressure-drop, and added to the tube with the least pressure-drop. It seems reasonable that Δm should be high when there is a big difference in pressure drop, that Δm should be smaller for longer tubes than shorter, and that Δm should be bigger for tubes with bigger diameter than for smaller diameter tubes.

With this iteration method the mass flow rates in only two tubes are updated in each iteration. This has the advantage that it's easy to respect the mass balance, and it's easy to implement. The disadvantage is that if there are big differences in external conditions in each tube the run time of the program increases significantly.

The tolerance is chosen as a relative tolerance of 10^{-3}, that is

$$tolerance = 10^{-3}\Delta p_{\max}$$

Equation 6.7-4

6.8 Outlet conditions

The outlet temperature, T_{out}, is a typical specification for a heat exchanger. If the temperature profiles are different in the tubes, the outlet temperature and mass fraction (if condensation occurs) in each tube will differ. If the mass flow rate is different in each tube T_{out} can't be obtained by a simple average of the outlet temperatures in each tube.

T_{out} is obtained from the total duty of the heat exchanger. The total enthalpy at the outlet is the total inlet enthalpy minus the total duty of the heat exchanger. T_{out} is obtained from interpolation at the total enthalpy at the outlet. The mass fraction at the outlet is then obtained by interpolating at the calculated outlet temperature.

The pressure in each tube should obviously be equal, but because of a finite tolerance level small deviations may occur. The outlet pressure is calculated from an average of the pressure drops.

6.9 Implementation of tube-side HTC

The value Z_g in Equation 4.6-1 is implemented as follows

$$Z_{g,i} = x_i c_{pg,i} \frac{T_i - T_{i-1}}{h_i - h_{i-1}}$$

Equation 6.9-1

If there is two-phase flow at the inlet the following approximation is used for Z_g at the inlet

$$Z_{g,1} = x_1 c_{pg,1} \frac{T_1 - (T_1 + 0.5)}{h_1 - h_{T_1+0.5}}$$

Equation 6.9-2

As mentioned before, choice of tube-side HTC in condensing flow must be done with care. It is possible to choose between the three mentioned correlations for two-phase flow (see 6.13).

The correlation by Gnielinski (Equation 4.4-5) is used for single-phase flow with Equation 4.4-6 for correction for rough tube walls. The silver method (Equation 4.6-1) is used for HTC in condensation of mixtures. For the HEDH correlation in two-phase flow, C_f from Equation 4.6-3 is used as enhancement factor on the gas-phase HTC, and the corrected Fuchs is used for calculating the interfacial shear force.

C_f is also implemented as enhancement factor for gas-phase HTC with the Boyko and Kruzhilin correlation for liquid HTC. The modification made by Neeraas is implemented so liquid film HTC is calculated from Equation A 10. The Thome correlation is used in its original form. The Dittus-Boelter correlation (Equation 4.4-4) is used for gas-phase HTC for both the HEDH and Boyko and Kruzhilin correlation. The liquid-only HTC in the Boyko and Kruzhilin correlation is calculated from Gnielinski (Equation 4.4-5) with correction for tube wall roughness.

6.10 Implementation of waterside HTC

For natural convection around horizontal tubes Equation 4.10-3 combined with Equation 4.10-4 is used. For natural convection around vertical tubes Equation 4.10-6 and Equation 4.10-8 are used for laminar and transition/turbulent respectively.

In forced convection in parallel flow Equation 4.11-3 and Equation 4.11-4 are used for laminar and turbulent flow, respectively. In cross flow Equation 4.11-1 is used. Equation 4.12-1 is consequently used for determining the combined HTC from natural and forced convection. The value of n is set equal to 4 as suggested by HEDH[**12**] and Cengel[**9**].

6.11 Transition from single-phase to two-phase

The transition from single-phase to two-phase flow is obtained by checking if the mass fraction of the vapor is between 0 and 0.99. At the transition there is a change in correlation for tube-side HTC. The HTC drops significantly for the test case (appendix C) (see Figure 4.7-1). This leads to a

discontinuity in the overall HTC and the outside wall temperature. Though it is not physically logic that the wall-temperature takes a sudden drop, it does not cause any problems for running the program in the current state. But generally, discontinuities can lead to that a program breaks down at the discontinuity. This can be dealt with by using single phase HTC down to x=0.95 for example, or using some kind of interpolation from x=1 to x=0.95 in order to get a smooth profile on the tube side HTC and the wall temperature.

Since the flow pattern at vapor fractions between 0.95 and 1 probably is liquid droplets entrained in the gas core, it seems logic to use single-phase expressions for tube side HTC down to x=0.95. The models used are for annular flow, and annular flow requires enough liquid to form a liquid film around the periphery of the tube.

6.12 Obtaining water temperature profile in counter-current flow

As mentioned before, the water temperature and tube-side fluid temperature are not known at the same position in countercurrent flow. Therefore, the water temperature at the tube-side inlet is guessed. This is only necessary in the closed case. A first guess is that the water temperature has a rise of 5 degrees. The water temperature at the tube outlet is then checked against the actual water temperature. If it's higher the guess is reduced, if it is lower the guess is heightened. This is repeated until the actual water temperature is reached at the outlet with a given tolerance. Figure 6.12-1 illustrates this iteration process.

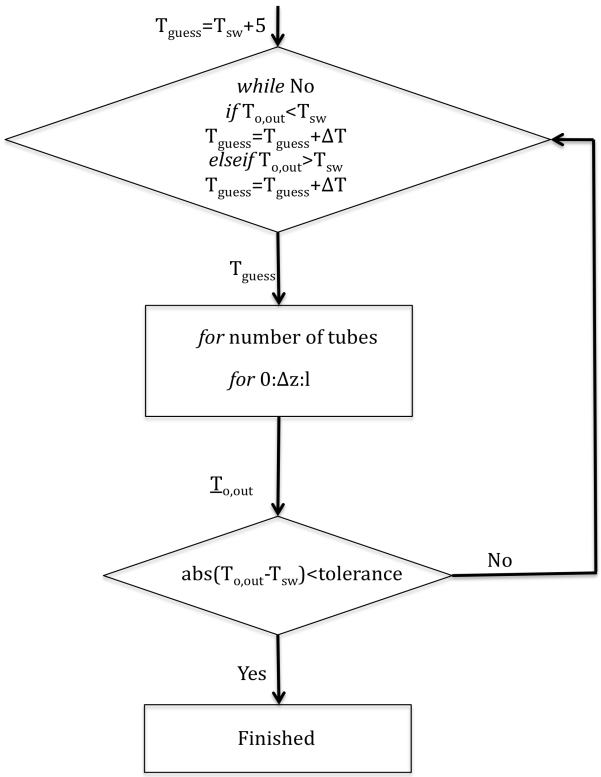

Figure 6.12-1 Iteration process for water temperature in countercurrent flow

The tolerance is set to 0.5 degrees. The ΔT should be chosen based on the difference between the calculated seawater temperature and the actual seawater temperature, but it's not chosen as the value of the difference because the heat transfer is affected by the temperature difference. It is chosen as half the difference between $T_{o,out}$ and T_{sw}.

$$\Delta T = abs(\frac{T_{o,out} - T_{sw}}{2})$$

Equation 6.12-1

Since the HTC in parallel flow is dependant on the local distance along the tube, and the distance outside the tube starts at the opposite end as the inside of the tube, the distance outside the tube must me implemented separately. This distance starts at zero at the outlet for the process fluid, and goes to the tube length at the inlet for the process fluid. This is illustrated in Figure 6.12-2.

Figure 6.12-2 Illustration of distances in parallel countercurrent flow

6.13 Running the program

The program is run from the m-file *heatex.* In *heatex* all necessary input parameters are set. Geometric parameters such as tube diameter, tube orientation, tube length, number of tubes and tube wall roughness must be specified. The thermal conductivity of the tube wall must also be specified.

The file where the thermodynamic and physical properties are must be specified. The MATLAB function *importfile* reads the file and saves the data into variables. Total mass flow rate, inlet temperature and inlet pressure are also specified.

In *heatex* the flow orientation of the seawater must be specified along with the seawater velocity and temperature. If a closed solution is desirable the water mass flow rate must be specified. If an open solution is desirable the mass flow should be specified as *Inf* (infinity). The water orientation is specified in the variable *waterorient* with different integers for the different orientations. What integer that corresponds to which water orientation is commented in the m-file. A constant outer HTC can be specified in the variable *hokonst*.

It is possible to choose between the three mentioned correlations for HTC inside tubes during condensation. This is done in the variable *mod. mod=1* for HEDH, 2 for the modified Boyko and Kruzhilin and 3 for Thome. A constant tube side HTC can also be specified. This is done by setting the variable *mod* equal to 4 and specifying the desired inner HTC in the variable *hikonst*. The step size (Δz) is also chosen in *heatex*. It is recommended to choose this value small compared to the tube length. 0.01% of the tube length is an okay value.

The combined fouling and coating resistance on the outside of the tubes is also set in *heatex.*

The outlet conditions, pressure-drop, duty and heat transfer area will be displayed in the MATLAB workspace when the program has finished.

7 Description of test cases

7.1 Introduction

In order to ensure that the calculation model works as desired, simulation of two test cases have been carried out. The test cases are connected through a hypothetical subsea compression system. One well stream cooler, where the cooler should condense out liquid for separation and one compressor after-cooler for pipeline transport are the basis for the test cases. The system is illustrated in Figure 7.1-1. The cooling capacity of the seawater is assumed to be infinite, so the seawater temperature is constant. The modified Boyko and Kruzhilin correlation is used for liquid HTC in two-phase flow.

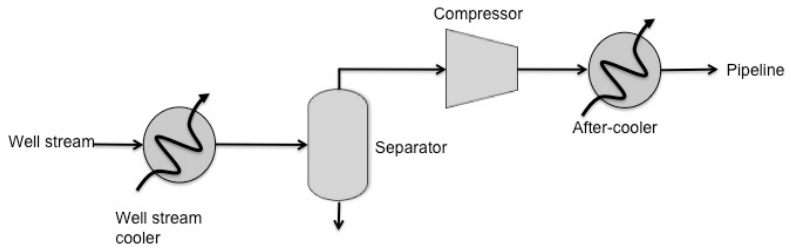

Figure 7.1-1 Hypothetical system for test cases

7.2 Well stream cooler case

The well stream cooler should cool a typical well stream for separation before compression of the gas and pumping of the liquid. The well stream composition is shown in Table 7.2-1. The well stream is mostly methane, but there are also some heavier hydrocarbons.

Component Name	Comp. Id.	Z [mol%]	MW [kg/kmol]
		100	23.48
Nitrogen	N2	2	28.016
Carbon Dioxide	CO2	5	44.01
Methane	C1	75	16.042
Ethane	C2	6	30.068
Propane	C3	5	44.094
I-Butane	IC4	2	58.12
N-Butane	NC4	2	58.12
I-Pentane	IC5	1	72.146
N-Pentane	NC5	1	72.146
Hexane	C6	0.5	86.172
Heptane	C7	0.5	96

Table 7.2-1 Composition of well stream

The inlet conditions are shown in Table 7.2-2.

T[C]	70
P[bar]	70
m[kg/s]	200

Table 7.2-2 Inlet conditions well stream

Two cases have been established for the well stream cooler. The outlet conditions for the two cases are shown in Table 7.2-3. Case 2 is for avoiding the formation of hydrates.

	Case 1	Case 2
Tout[C]	9	25
max ΔP [bar]	0.5	0.5

Table 7.2-3 Outlet conditions for well stream

Figure 7.2-1 shows the phase envelope for the fluid with the inlet and outlet conditions. 1 denotes inlet, 2 denotes outlet case 2, and 2' denotes outlet case 1. In both cases the outlet condition is in the two-phase region. This ensures that the model is tested in the two-phase area.

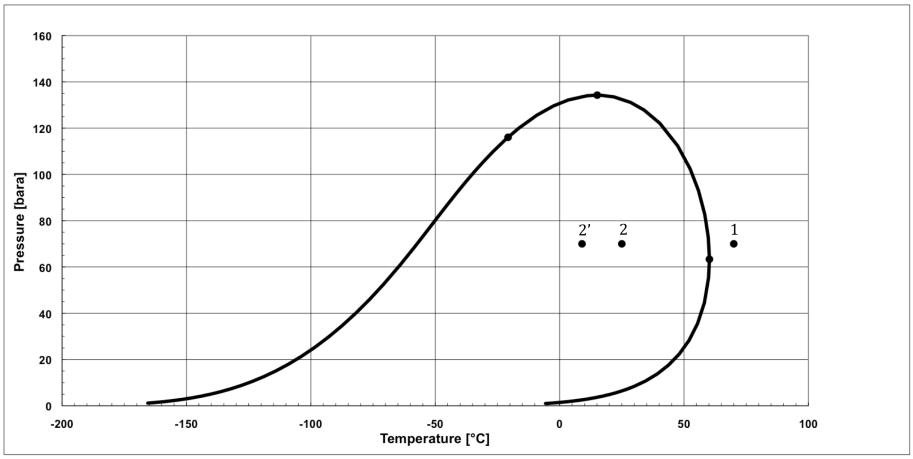

Figure 7.2-1 Well stream phase envelope with inlet (1) and outlet conditions (case 1 (2'), case 2 (2))

The water temperature is 5 C and the maximum seawater velocity is assumed to be 1 m/s. Horizontal two-inch tubes are used for both cases, but in case 2 a design with one-inch tubes is also carried out. Geometric tube specifications are shown in Table 7.2-4.

Tube	1 inch	2 inch
Do[m]	3.34E-02	6.03E-02
Wall thickness[m]	3.38E-03	3.91E-03

Table 7.2-4 Geometric tube specifications [27**]**

A conservative design, i.e. only natural convection, is carried out for both cases. In case 2 a sensitivity study is carried out. The sensitivity parameters are flow rate of well stream, combined forced and free convection on the waterside, and tube orientation, vertical or horizontal.

A typical roughness for stainless steel tubes is used together with a typical thermal conductivity. These are shown in Table 7.2-5.

e[m]	2.00E-06
λ_w[W/mK]	15

Table 7.2-5 Tube wall roughness and thermal conductivity [7**][**9**]**

7.3 After-cooler case

The gas flow rate from the well stream case 2 is used for the after-cooler case. This is a lighter fluid because some of the heavier hydrocarbons have been removed. The composition is shown in Table 7.3-1

Component Name	Comp. Id.	Z [mol%]	MW [kg/kmol]
		100	22.31
Nitrogen	N2	2.0	28.02
Carbon Dioxide	CO2	5.0	44.01
Methane	C1	77.5	16.04
Ethane	C2	5.9	30.07
Propane	C3	4.5	44.09
I-Butane	IC4	1.6	58.12
N-Butane	NC4	1.5	58.12
I-Pentane	IC5	0.8	72.15
N-Pentane	NC5	0.6	72.15
Hexane	C6	0.3	86.17
Heptane	C7	0.3	96.00

Table 7.3-1 Composition after-cooler case

The inlet conditions are shown in Table 7.3-2. The pressure and temperature is increased through the compressor, but a reduction in mass flow rate because of the separation of liquid.

T[C]	80
P[bar]	100
m[kg/s]	172

Table 7.3-2 Inlet conditions after cooler

A design with the same two-inch tubes as used in the well stream cases (see Table 7.2-4 and Table 7.2-5) is carried out. The outlet temperature and pressure drop are as in well stream case 1, 9 C and 0.5 bar. The phase envelope with inlet (1) and outlet (2) conditions for the fluid is shown in Figure 7.3-1. At the outlet condition there is some liquid.

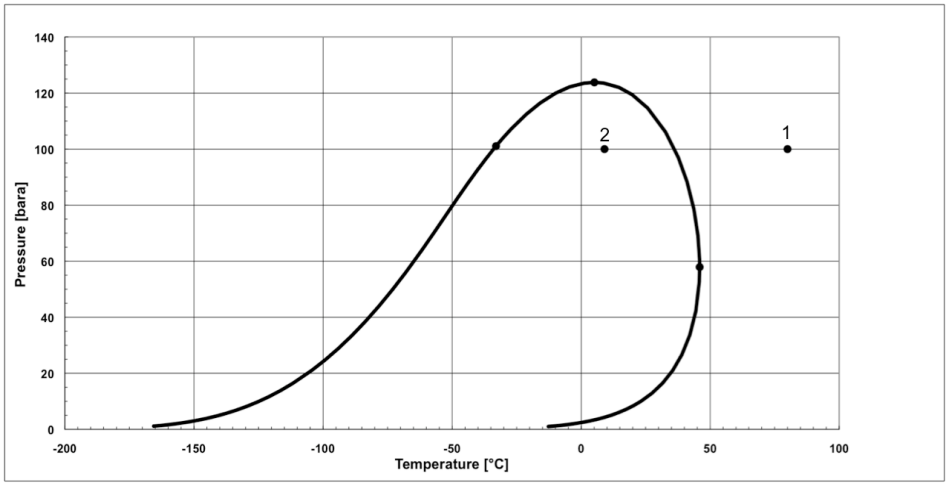

Figure 7.3-1 Phase envelope after-cooler fluid with inlet (1) and outlet (2) conditions

8 Results and discussion

8.1 Well stream cooler case 1

This design has very low driving forces at the outlet since the temperature difference is only 4 C. In addition the HTC on the outside decreases with decreasing temperature difference between tube wall and the seawater. The combination of these two leads to huge heat transfer area requirements at the cold side of the cooler. This is illustrated in Figure 8.1-1 for one tube. This shows that a 160 m long tube is needed for achieving the desired outlet temperature for this particular tube mass flux.

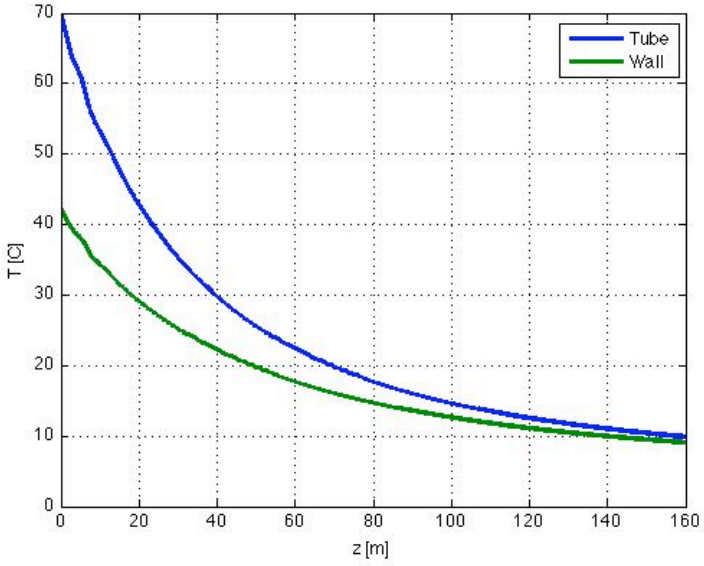

Figure 8.1-1 Temperature profile well stream case 1, G=369.83 kg/m²s

There is nothing to gain by increasing the mass flux in each tube, because most of the resistance is on the outside. This is illustrated in Figure 8.1-2. The tube side HTC and pressure drop will increase if the mass flux in each tube is increased, but the overall HTC won't be affected very much. The allowed pressure drop can't be utilized for increasing the heat transfer.

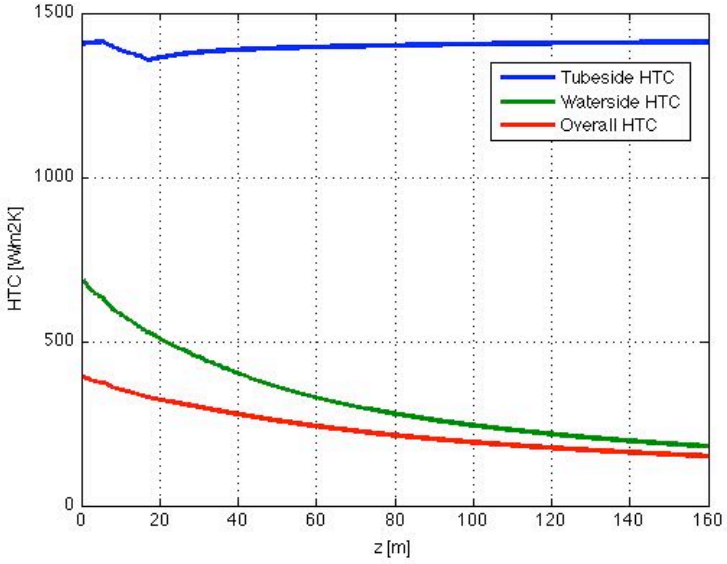

Figure 8.1-2 HTC well stream case 1, G=369.83 kg/m²s

Based on this discussion the design is just dependant on what is the most practical of fewer longer tubes or many shorter tubes. A design has been made that is a compromise. The design is as described in Table 8.1-1.

Duty [MW]	**39**
Tout [C]	**9.49**
ΔP [bar]	**0.38**
Tubes [-]	**250**
Tube length [m]	**160**
Total area [m2]	**7577.5**

Table 8.1-1 Design well stream case 1

The outlet temperature is not reached. The area requirements for the last half-degree is very big. The max allowed pressure drop is not utilized. This would have lead to fewer and longer tubes.

The design made here is not a suitable design. 250 tubes of 160 meters each are not practical. Construction and transportation of such a cooler would be very difficult and very expensive. A conclusion that can be drawn from this is that passive coolers that rely solemnly on natural convection are not suitable if a small temperature difference at the outlet is required. The allowed pressure drop could instead be used through a combined expander/pump for generating motion on the seawater around the outlet.

8.2 Well stream cooler case 2

At the mass flux chosen for case 1 the required tube length can be estimated from Figure 8.1-1. At the same mass flux 250 tubes of roughly 50 meters is required. But in order to utilize the allowed pressure drop and for decreasing the number of tubes the mass flow in each tube is increased. Based on the trial and error procedure the design with two-inch tubes are as stated in Table 8.2-1.

Duty [MW]	**28.5**
Tout [C]	**24.5**
ΔP [bar]	**0.43**
Tubes [-]	**160**
Tube length [m]	**70**
Total area [m2]	**2121.7**

Table 8.2-1 Design well stream case 2 - 2 inch tubes

The temperature profiles are shown in Figure 8.2-1.

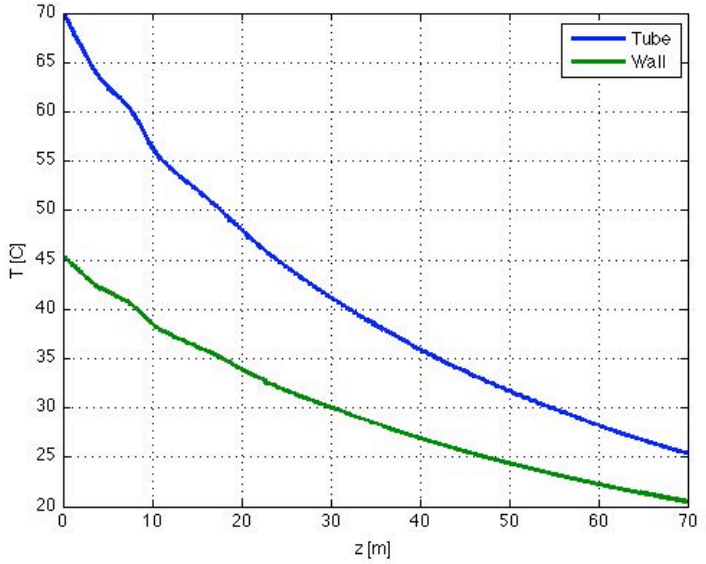

Figure 8.2-1 Temperature profile well stream case 2 - 2 inch tubes, G=577.87 kg/m²s

Figure 8.2-2 shows the tubeside, outside and overall HTCs. The tubeside HTC is higher compared to case 1 due to the higher mass flux, but the overall HTC is not affected because the waterside HTC is much smaller than the tubeside.

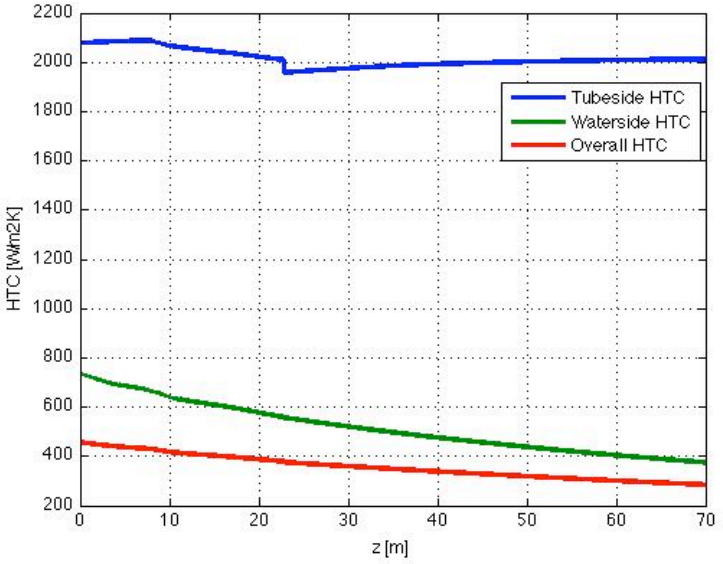

Figure 8.2-2 HTC well stream case 2- 2 inch tubes, G=577.87 kg/m²s

This design is more realistic. The area is decreased with 72% compared to the case with 9 C at the outlet, but the duty is only decreased with 27%. This illustrates how much the area requirements increase as the temperature difference decreases.

The design with one-inch tubes is shown Table 8.2-2. The allowed pressure drop was utilized in this design as well. The important difference between the one-inch and two-inch design is the tube length and the number of tubes. The total area is pretty similar but it is distributed differently. The one-inch design allows shorter tubes, but requires 3.7 times more tubes. This is a trade-off that must be considered when deciding which tubes are best suited.

Duty [MW]	**28.4**
Tout [C]	**24.7**
ΔP [bar]	**0.5**
Tubes [-]	**588**
Tube length [m]	**33**
Total area [m2]	**2036.1**

Table 8.2-2 Design well stream case 2- 1 inch tubes

Figure 8.2-3 shows the temperature profiles with the one-inch tubes.

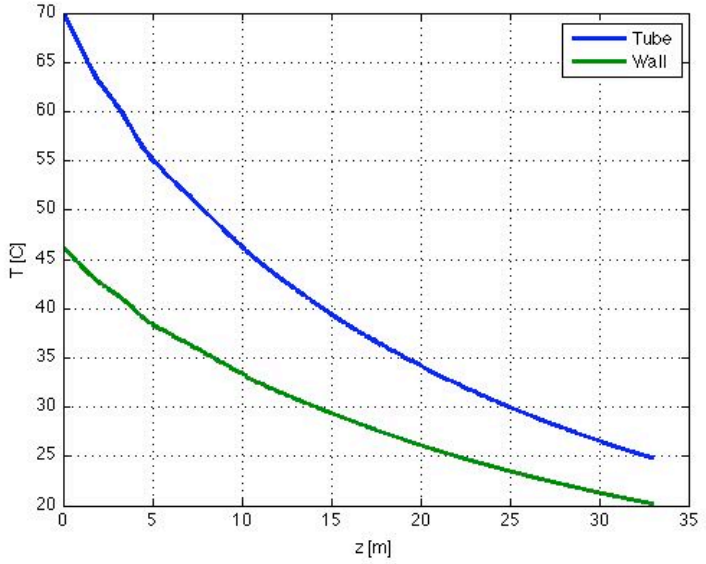

Figure 8.2-3 Temperature profile well stream case 2 - 1 inch tubes, G=609.99 kg/m²s

Figure 8.2-4 shows the HTCs. The tubeside HTC is higher for the one-inch tubes compared to the two-inch tubes due to the higher mass flux, but as discussed previously this does not affect the overall HTC considerably.

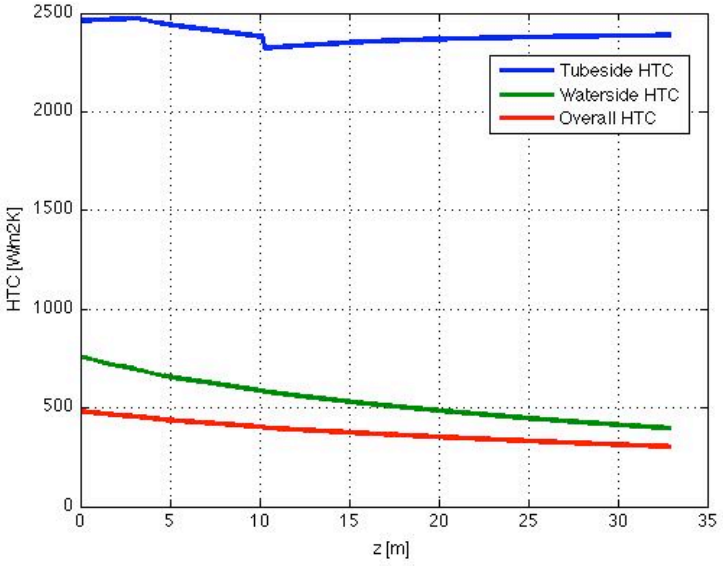

Figure 8.2-4 HTC well stream case 2- 1 inch tubes, G=609.99 kg/m²s

8.3 Sensitivity on well stream case 2

8.3.1 Seawater velocity and direction

As discussed in section 4.12 the seawater velocity influences the waterside HTC considerably. Figure 8.3-1 shows the outlet temperature of the one-inch tube design in parallel and cross flow as a function of seawater velocity. In cross flow the outlet temperature drops significantly even at low seawater velocities. But at about vsw=0.3 the profile straightens out. This is because the constraining HTC shifts from the outside to the inside. So it is the tube side HTC that is the constraining HTC. In parallel flow the outlet temperature decreases more steadily. This shows that the waterside HTC still is the constraining HTC even at sweater velocities at 1 m/s.

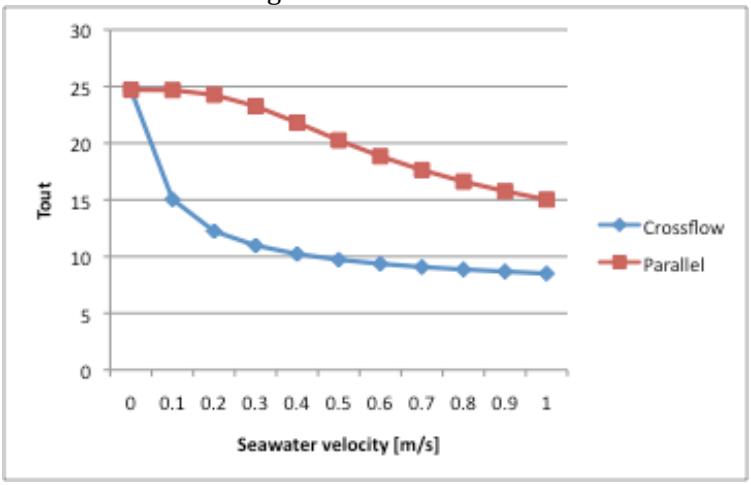

Figure 8.3-1 Outlet temperature vs seawater velocity in cross flow and parallel flow - one-inch tube design

The pressure drop is not affected very much by the change in seawater velocity. A small decrease in pressure drop is experienced because of the fact that more liquid is formed which leads to a lower two-phase velocity. A similar study has been carried out on the two-inch design, and the results are very similar. There was no extra "diameter-effect".

This discussion shows that the seawater velocity influences the outlet temperature significantly. In addition the direction of the seawater affects the outlet temperature.

8.3.2 Feed flow rate

During production it will be necessary to decrease the flow rate because of unforeseen situations or during start-up and shutdown. It's interesting to see how the cooler responds to such changes in flow rate. The feed flow rate

has been varied between 50 and 100 % of design flow rate. Figure 8.3-2 shows the outlet temperature with decreasing mass flow rates for the one-inch tube design. The effect from the reduction in mass flow rate on the outlet temperature is not as strong as the case was for cross flow forced convection. The tubeside HTC becomes lower with decreasing mass flow, but it is still the outer HTC that is the constraining one. The reduction in outlet temperature is because there is less mass in each tube to cool down.

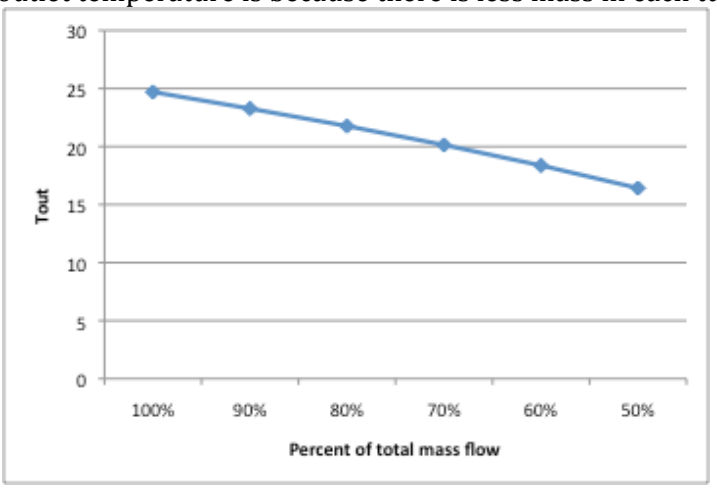

Figure 8.3-2 Outlet temperature as a function of decrease in total mass flow rate, one inch tube

The reduction in mass flow rate has a very strong effect on the pressure drop. This is illustrated in Figure 8.3-3. The reduction in pressure drop is caused by the reduction in velocity. The low pressure-drops can induce maldistribution.

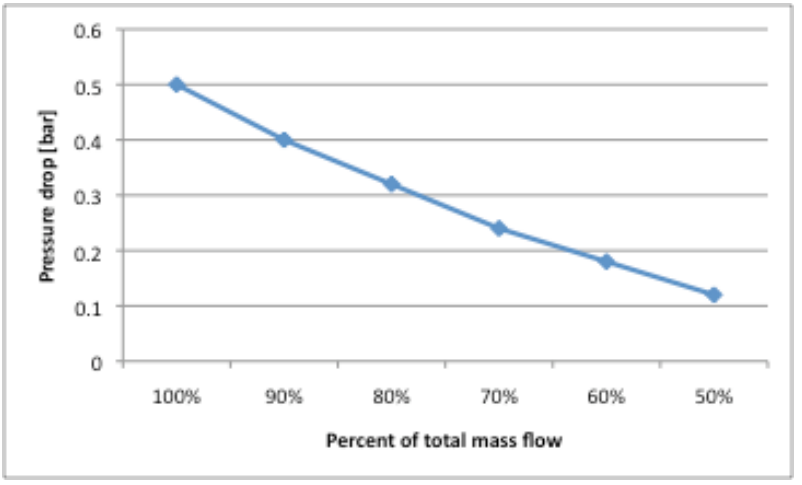

Figure 8.3-3 Pressure drop as a function of decrease in total mass flow rate, one-inch tube

8.3.3 Tube orientation

The designs so far have been with horizontal tubes. An advantage with vertical tubes is that the seawater velocity will always be perpendicular to the tube orientation, so the tubes will always be in cross flow when there is motion in the seawater. This makes it easier to predict the heat transfer. On the other hand, the pressure drop will increase due to the change in static height. Table 8.3-1 shows the outlet conditions and design if the one-inch cooler design is placed vertically instead of horizontally.

Duty [MW]	27.9
Tout [C]	25.5
ΔP [bar]	0.76
Tubes [-]	588
Tube length [m]	33
Total area [m2]	2036.1

Table 8.3-1 One-inch tube design with vertical tubes

The outlet temperature is not changed significantly; this shows that the outer HTC on vertical tubes are quite similar to horizontal tubes. The difference is that the boundary layer increases along the tubes. The pressure drop increases with 52%. The increase is due to the gravitational pressure drop. The pressure drop increases more with the two-inch tubes because of the longer tubes.

8.3.4 Worst case

The worst case in this sensitivity study is 50% flow rate and seawater in cross flow at 1 m/s. Simulations of both the one-inch and two-inch design shows that the outlet temperature is 6 degrees if worst case is encountered. Six degrees is only one degree above the seawater temperature. This illustrates how the effects of varying operating conditions influence the performance of the cooler.

8.3.5 Summary of sensitivity on well stream cooler case 2

The designed heat exchangers performances are very sensitive to seawater velocity. The outlet temperature can become significantly lower, especially in seawater cross flow. The designs are not very sensitive to tube orientations, but if placed vertically only cross flow is experienced, and this makes it easier to predict. The mass flow rate sensitivity is actually relatively small, except the obvious sensitivity because of less mass to cool. This is because the overall HTC is not very sensitive to mass flow rate, because the resistance is on the outside of the tubes.

8.4 After-cooler

A similar design procedure as in the previous cases was carried out. A design that meets the requirements is shown in Table 8.4-1.

Duty [MW]	37.6
Tout [C]	9.07
ΔP [bar]	0.49
Tubes [-]	172
Tube length [m]	220
Total area [m2]	7168.4

Table 8.4-1 Design after-cooler

The required heat transfer area is very large. 172 tubes of 220 meters is not easily manufactured and transported. The reason for the huge area requirements is, as the case was for the well stream cooler case 1, the small temperature difference at the outlet. Small driving forces and a low HTC leads to big area requirements. The temperature profiles are shown in Figure 8.4-1. At approximately half the tube length 92% of the temperature drop has been achieved. This means that 50% of the heat transfer area is used for the last 8% of the temperature drop. At the outlet the outer wall temperature and the fluid temperature are almost equal.

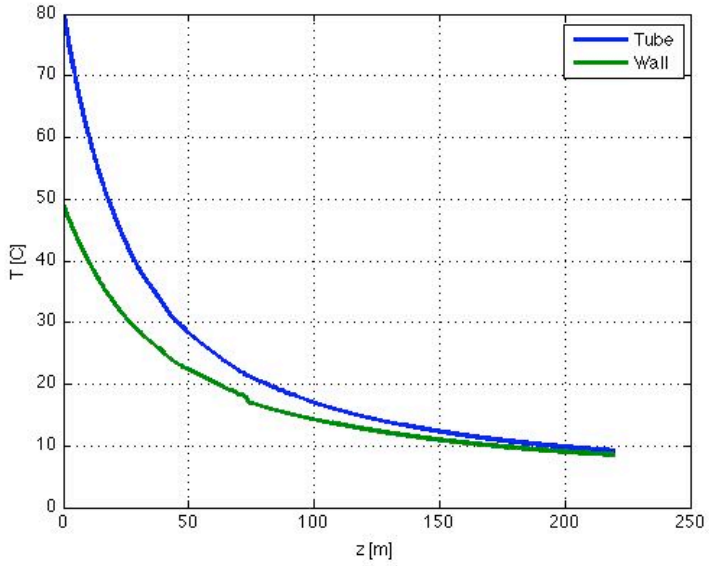

Figure 8.4-1 Temperature profile after-cooler, G=462.30 kg/m²s

The various HTCs are shown in Figure 8.4-2. The tube side HTC drops from approximately 1950 W/m²K to approximately 1450 W/m²K at z≈75 m. The drop is caused by transition from single-phase to two-phase. This is a 25%

drop, but the overall HTC only experiences a small drop. At the outlet the overall HTC and the waterside HTC are almost equal.

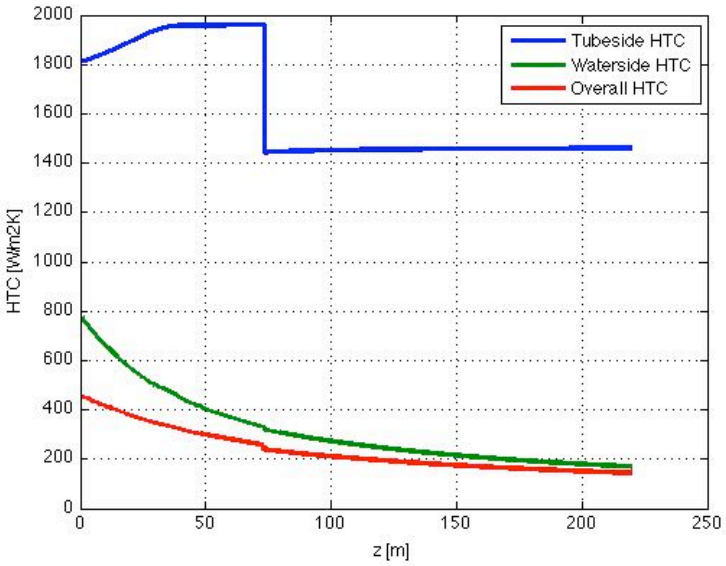

Figure 8.4-2 HTC after-cooler, G=462.30 kg/m²s

8.5 Sensitivity after-cooler

A sensitivity study is carried out on the after-cooler. The same parameters that were changed in the sensitivity-study of well stream case 2 are changed.

8.5.1 Seawater velocity and direction

In cross flow the outlet temperature reaches the seawater temperature when there is any motion at all in the seawater. In parallel seawater flow the outlet temperature decreases more steadily. This is illustrated in Figure 8.5-1. Only small deviations in pressure drop were experienced.

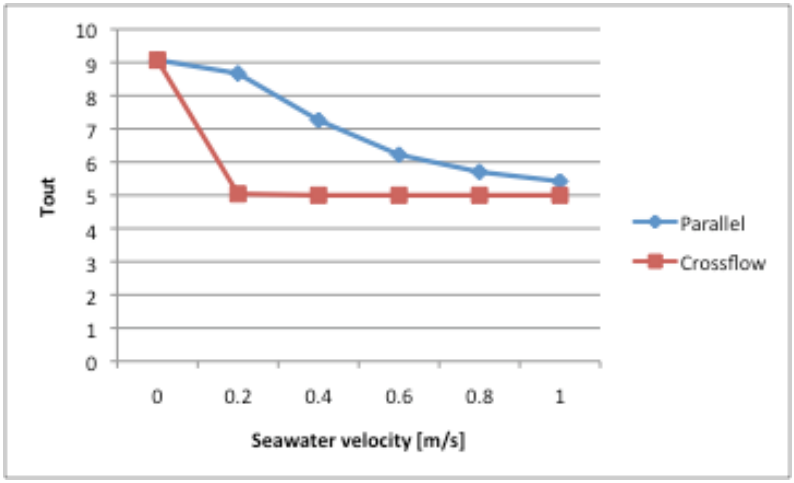

Figure 8.5-1 Outlet temperature in parallel and cross flow for after-cooler

8.5.2 Feed flow rate

Figure 8.5-2 shows the outlet temperature at reduced mass flow rates. The outlet temperature is, as expected, reduced as the mass flow rate is reduced. The linearity of the profile suggests that it is only the reduction in mass that causes the drop in outlet temperature, and not any significant changes in overall HTC.

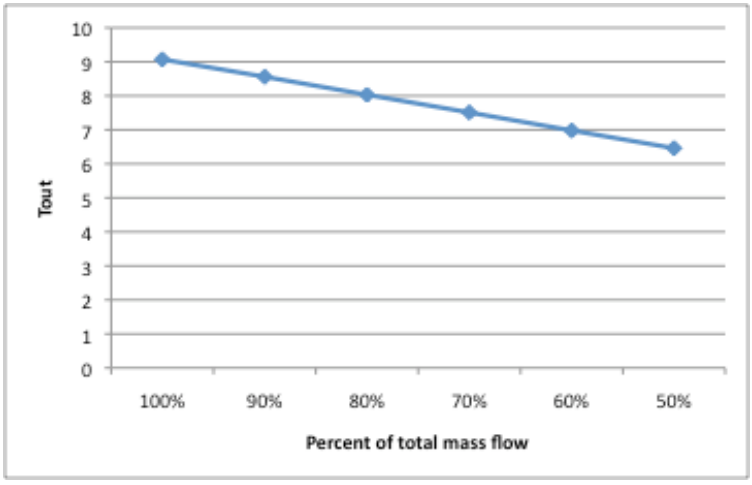

Figure 8.5-2 Outlet temperature as a function of reduction in mass flow rate in after-cooler

Figure 8.5-3 shows the pressure drop at reduced mass flow rates. As expected the pressure drop decreases as the mass flow rates decreases due to the lower velocity in the tubes.

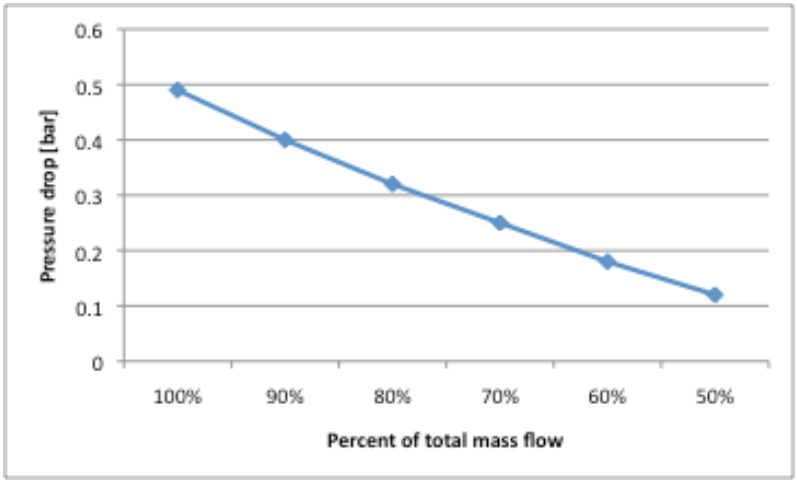

Figure 8.5-3 Pressure drop at reduction in mass flow rate in after-cooler

8.5.3 Tube orientation

The outlet temperature increases with half a degree if the tube orientation is vertical instead of horizontal. The pressure drop increases substantially because of the long tubes and the big height difference. The pressure-drop increases to 3.32 bar. This is a 564% increase in pressure-drop, but in reality tubes of this length will have bends. The bends would make some parts of the tubes vertically oriented and some parts horizontally oriented.

8.5.4 Summary of sensitivity for after-cooler

The outlet temperature is not very sensitive to changes in operational conditions. This is because the outlet temperature is only 4 degrees higher than the seawater temperature in the design case. The pressure drop in the designed cooler is very sensitive to tube orientation because of the long tubes that cause a big drop in static pressure if placed vertically.

8.6 Summary of test cases

Four coolers have been designed, three designs as well stream cooler and one design as compressor after-cooler. The area requirements for subsea heat exchangers that rely on natural convection are very large. Especially in the cases where there is a small temperature difference at the outlet. This small temperature difference leads to low driving forced and low overall HTC. Sensitivity studies were carried out on the well steam cooler with 25 C outlet temperature, and on the after-cooler. The well stream cooler outlet temperature is very sensitive to external conditions, but overall HTC only experience a small sensitivity to reduction in feed flow rate. The after-cooler outlet temperature is not very sensitive to either reduction in mass

flow rate or external conditions. Because of the long tubes the pressure drop is very sensitive to tube orientation due to the drop in static pressure.

The designs made for the coolers with 9 C at the outlet require a great heat transfer area. This introduces great challenges in production and transportation. On the other hand, there are basically no constraints on the size with regards to space on the seabed. The coolers with the low temperature difference at the outlet are very robust to changes in operational conditions, which is an advantage.

An important factor for the designs is the seawater velocity. The designs made here are conservative designs. In reality, there could be motion in the seawater continuously. If that is the case, the conservative design overestimates the required heat transfer area greatly. In future designs an average seawater velocity could be used. A measure for generating motion in the seawater around the tubes could be used when necessary. This would lead to a much more compact heat exchanger, but the trade-off is the added complexity because of the measure for generating motion.

9 Experiences and possible improvement of calculation model

The calculation model in its current state is a first version and that must be kept in mind. Even though the calculation model is usable now, improvements can be made for a more efficient program and it can be expanded to account for additional aspects.

In general the program works as desired. Heat exchangers for subsea applications can be designed with this program. It's easy to set and change the parameters, which makes the functionality of the program good. Studies on influence of the different parameters are easily carried out.

The run-time of the program can be improved. As shown in the test cases very long tubes may be required, and this leads to long run-time. A possible improvement is to change the step–size (Δz) based on the temperature gradient. At low temperature gradients a longer step size could be used for decreasing the run-time.

The only problem encountered when running the program is that the function *twallstart* does not always find the wall temperature at the inlet. This is dependant on the chosen step size and the tolerance level. The problem is easily solved through decreasing the step size or increasing the tolerance level.

The model developed in this study is for straight parallel tubes. As mentioned earlier, bends will make the design more compact. By introducing bends the pressure drop increases on the tube side, and this must be accounted for by pressure loss coefficients. By introducing bends in a closed heat exchanger where the water temperature varies from layer to layer, the calculation procedure should be divided into segments. But the model in its current state can be used as basis for each segment, except the segment where the bends are. In a closed arrangement baffles may also be used on the waterside for leading the flow and induce turbulence. But other commercial software exists for calculating traditional shell and tube heat exchangers.

A natural expansion of the model is to include an equation of state. Currently, the user must specify thermodynamic and physical properties in tables. A future version of the program should include an equation of state so that the user only specifies composition, and the properties are

calculated from the equation of state. This would make he model easier to use in the sense that property tables does not to have to be produced.

Another measure for making the program user-friendlier is a graphical interface for the user. An interface where the user can specify geometric specifications and other inlet conditions is desirable. An .exe-file should be made for running of the program. This would give the program a more commercial look.

In commercial software for designing heat exchangers the program automatically iterates until the specifications are reached. For example, allowed pressure drop, size and outlet temperature are specified and the program iterates until the specifications are reached. Since this is the first version of the program all problems/flaws may not have been encountered or found yet. Therefore, such an iteration loop has not been included. When it is established that the program functions as desired this should be implemented.

10 Conclusion

A calculation model for a subsea heat exchanger has been developed. The model is implemented in the commercial software MATLAB. The model is based on straight tubes that can be horizontally or vertically oriented. Different orientations of the surrounding seawater are implemented in the model.

Heat transfer and frictional pressure drop correlations have been studied, and based on this study the modified Boyko and Kruzhilin correlation is recommended for heat transfer coefficient in condensing two-phase flow inside tubes and the corrected Fuchs correlation is recommended for calculation of frictional pressure drop in two-phase flow inside tubes.

The model has been tested on two test cases: one test case for simulating a well stream cooler, and one for simulation of an after-cooler in a subsea compression system. Experiences from simulation of two test cases show that the model is suited for design, and parameter sensitivity studies, of subsea heat exchangers.

11 Bibliography

[1] T. Bjørge and L. Brenne, Subsea gas compression; Available technology and future needs, February 2008.

[2] (2006, March) Wikimedia Commons. [Online]. http://commons.wikimedia.org/wiki/File:Straight-tube_heat_exchanger_1-pass.PNG

[3] B. Van Der Rest, "Subsea Heat Exchanger," PCT/NO2009/000248, July 3, 2008.

[4] V. Sten-Halvorsen, E. Baggerud, and T. Hollingsæter, "Subsea Cooler," PCT/NO2008/000196, Juni 01, 2007.

[5] J. El Hajal, J. R. Thome, and A. Cavallini, "Condensation in horizontal tubes, part 1: two-phase flow pattern map," *Int. J. Heat and Mass transfer*, vol. 46, pp. 3349-3363, 2003.

[6] N. Kattan, J. R. Thome, and D. Favrat, "Flow boiling in horizontal tubes: Part 1 - Development of a diabatic two-phase flow pattern map," *Trans. ASME*, vol. 120, pp. 140-147, 1998.

[7] F. M. White, *Fluid Mechanics*, 6th ed.: McGraw Hill, 2008.

[8] S. E. Haaland, "Simple and explicit formulas for the friction factor in turbulent pipe flow," *J. Fluids. Eng*, pp. 89-90, 1983.

[9] Y. A. Cengel, *Heat and mass transfer - A practical approach*, 3rd ed., Y. A. Cengel, Ed.: McGraw-Hill, 2006.

[10] V. Gnielinski, "New equations for heat and mass transfer in turbulent pipe and channel flow," *Int. Chem. Eng.*, vol. 16, pp. 359-368, 1976.

[11] B. S. Pethukov, "Advances in heat transfer," vol. 6, 1970.

[12] G. F. Hewitt, *Heat Exchanger Design Handbook*.: Hemisphere publishing corporation, 1983.

[13] R. H. Norris, "Augmentation of convection heat and mass transfer," *American society of mechanical engineers*, 1971.

[14] W. Nusselt, "Die Oberflachenkondensation des Wasser-dampfes," *Zeitschr. Ver. Deutch. Ing*, vol. 60, pp. 541-569, 1916.

[15] B. O. Neeraas, *Condensation of hydrocarbon mixtures in coil-wound LNG heat exchangers*.: Department of refrigeration engineering (NTNU), 1993, Doctor thesis.

[16] J. R. Thome, J. E. Hajal, and A. Cavallini, "Condensation in horizontal tubes, part 2: new heat transfer models based on flow regimes," *Int. J.*

heat and mass transfer, vol. 46, pp. 3365-3387, 2003.

[17] B. C. Price and J. K. Bell, "Design of binary vapor condensers using the Colburn-Drew analogy," *AIChE symp. series*, vol. 70, no. 138, pp. 163-171, 1974.

[18] D. Del Col, A. Cavallini, and J. R. Thome, "Condensation of zeotropic mixtures in horizontal tubes: New Simplified Heat Transfer Model Based on Flow Regimes," *J. Heat Transfer*, vol. 127, pp. 221-230, 2005.

[19] P. H. Fuchs, "Pressure drop and heat transfer during flow of evaporating liquid in horizontal tubes and bends," *PhD thesis*, 1975.

[20] G. Hetsroni, G. F. Hewitt, J. M. Delhaye, and A. Lieberman, "Measurement techniques," in *Handbook of multiphase systems*, Gad Hetsroni, Ed.: McGraw-Hill Book Company, 1982, pp. 10-1 - 10-180.

[21] R. W. Lockhart and R. C. Martinelli, "Proposed correlation of data for isothermal two-phase, two-component flow in pipes," *Chem. Eng. Prog*, vol. 45, pp. 39-48, 1949.

[22] D. Chisholm, "Pressure gradients due to friction during the flow of evaporating two-phase mixtures in smooth tubes and channels," *Int. J. Heat mass transfer*, vol. 16, pp. 347-348, 1973.

[23] L. Friedel, "Improved friction pressure drop correlation for horizontal and vertical two-phase pipe flow," *Europeam two phase flow group meet., Ispra, Italy*, p. paper E2, 1979.

[24] V. K. Patnana, R. P. Bharti, and R.P. Chhabra, "Two-dimensinal unsteady flow of power-law fluids over a cylinder," *Chem. Engin. Science*, vol. 64, pp. 2978-2999, 2009.

[25] Various, *Compendium in TEP-07- Industrial heat engineering*.: Department of energi and process technology (NTNU), 2009.

[26] J. B. Aarseth, *Numerical calculation methods (In norwegian)*.: Department of construction-NTNU, 2008.

[27] Norwegian Steel Association. Norsok. [Online]. http://www.standard.no/norsok/L-001/pclass/FD30.htm

[28] D. Butterworth, "Simplified methods for condensation on a vertical surface with vapor shear," *UKAEA*, 1981.

[29] E. P. Anandiev, L.D. Boyko, and G.N. Kruzhilin, "Heat transfer in the presence of steam condensation in a horizontal tube," *Int. Heat transfer conf.* , vol. 2, pp. 290-295, 1961.

[30] B. O. Neeraas, Personal communication, 2010.

Appendices

A. Heat transfer correlations

The Heat Exchanger design handbook correlation:
This correlation is based on annular flow, or shear dominated flow. HEDH [**12**] suggest a correlation developed by Butterworth [**28**]. A critical liquid Reynolds number is defined based on the interfacial shear force. The liquid Reynolds number is defined as:

$$\mathrm{Re}_l = \frac{GD(1-x)}{\mu_l}$$

Equation A 1

The dimensionless shear force is defined as:

$$\tau_I^+ = \frac{\rho_l \tau_I}{(\rho_l^2 \mu_l g)^{2/3}}$$

Equation A 2

For $\tau^+ < 9.04$ the critical Reynolds number is given as:

$$\mathrm{Re}_c = 1600 - 226\tau_I^+ + 0.667(\tau_I^+)^3$$

Equation A 3

and for $\tau^+ > 9.04$, the critical Reynolds number is 50. If the Reynolds number is below the critical Reynolds number the HTC is given as:

$$\alpha^+ = 1.41\mathrm{Re}_l^{-1/2}(\tau_I^+)^{1/2}$$

Equation A 4

and for Reynolds numbers above the critical Reynolds number the HTC is:

$$\frac{\alpha^+}{(\tau_I^+)^{1/2}} = \left[(1.41\mathrm{Re}_l^{-1/2})^m + (0.071\mathrm{Pr}^{1/2}\,\mathrm{Re}^{-1/24})^m\right]^{1/m}$$

Equation A 5

Where m=0.5(Pr+3). The dimensionless HTC is defined as follows

$$\alpha^+ = \frac{\alpha}{\lambda_l}\left(\frac{\upsilon_l^2}{g}\right)^{1/3}$$

Equation A 6

This model needs calculation of the interfacial shear force. The simplest way of calculating it is to take [**12**]:

$$\tau_I = \frac{D}{4}\left(-\frac{dp_f}{dz}\right)$$

Equation A 7

The modified Boyko and Kruzhilin correlation:

Neeraas [**15**] made a modification to the original Boyko and Kruzhilin correlation [**29**]. Boyko and Kruzhilin's correlation has no empirically determined constants and is therefore interesting. The original correlation is given as:

$$\alpha = \alpha_{lo}(1 + x(\frac{\rho_l}{\rho_g} - 1))^{0.5}$$

Equation A 8

Neeraas modified it based on his experiments with propane. He proposed a correction factor:

$$k_\alpha = (1.15 - 0.275x)^{-1}$$

Equation A 9

So that the new expression for HTC is

$$\alpha = k_\alpha \alpha_{lo}(1 + x(\frac{\rho_l}{\rho_g} - 1))^{0.5}$$

Equation A 10

α_{lo} is calculated as if the liquid occupies all of the tube and is referred to as "liquid only". The liquid only Reynolds number is defined as:

$$\mathrm{Re}_{lo} = \frac{GD}{\mu_l}$$

Equation A 11

Equation 4.4-4 or Equation 4.4-5 can then be used for calculating α_{lo}. The mass flux in the experiments with propane ranges from 150-350 kg/m^{2}s, pressures between 12 and 20 bar, and vapor fractions between 0.15-0.88.

Thome's correlation:

Thome et al [**16**] developed a new correlation based on flow regimes. Their objective was to develop a new correlation with a minimum of experimentally determined constants. The correlation was compared to data points from 15 fluids, including n-butane, iso-butane, propylene and propane, which are hydrocarbons. The other fluids are the single component refrigerants R-11, R-12, R-22, R-32, R-113, R-125, R134a, R236ea, and the binary azeotropic mixtures R-32/R-125 (60%/40%), R404A and R-410A. The range of mass fluxes is 24-1022 kg/m^{2}s, vapor fractions in the range from 0.03 to 0.97, reduced pressures in the range from 0.02 to 0.80. 921 of 2771 data points in total are hydrocarbons data points.

Since it is based on flow regimes the expression for HTC differs from flow regime to flow regime. Here only the model for the annular flow regime will be presented. The expression for HTC for annular flow is

$$\alpha = 0.003\,\mathrm{Re}_l^{0.74}\,\mathrm{Pr}_l^{0.5}\,\frac{\lambda_l}{\delta}\,f_i$$

Equation A 12

Where δ is the film thickness and f_i is an interfacial roughness correction factor. The resemblance to the Dittus-Boelter equation is obvious but with the diameter replaced with the film thickness and a correction factor for the interfacial roughness. The constants in Equation A 12 are determined empirically from the HTC database.

In order to use Equation A 12 the film thickness needs to be calculated, which again requires calculation of void fraction. Void fraction is defined as

$$\varepsilon = \frac{A_g}{A} = \frac{A - A_l}{A}$$

Equation A 13

Film thickness is calculated from geometry from Equation A 14

$$\delta = \frac{D}{2} - \frac{\sqrt{\varepsilon D^2}}{2}$$

Equation A 14

Thome et al [**16**] used a void fraction model that is a logarithmic mean between the homogenous model (phases move with the same velocity, Equation A 15) and the model from Rouhani and Axelsson, which is a non-homogenous model [**16**] (Equation A 16). The Rouhani and Axelsson void fraction equation is based on the drift flux model.

$$\varepsilon_h = \left[1 + \left(\frac{1-x}{x}\right)\left(\frac{\rho_g}{\rho_l}\right)\right]^{-1}$$

Equation A 15

$$\varepsilon_{ra} = \frac{x}{\rho_g}\left(\left[1 + 0.12(1-x)\right]\left[\frac{x}{\rho_v} + \frac{1-x}{\rho_l}\right] + \frac{1.18(1-x)\left[g\sigma(\rho_l - \rho_g\right]^{0.25}}{G\rho_l^{0.5}}\right)^{-1}$$

Equation A 16

The logarithmic mean gives the following expression for the void fraction:

$$\varepsilon = \frac{\varepsilon_h - \varepsilon_{ra}}{\ln \frac{\varepsilon_h}{\varepsilon_{ra}}}$$

Equation A 17

The interfacial roughness correction factor proposed by Thome et al is calculated from Equation A 18.

$$f_i = 1 + \left(\frac{v_g}{v_l} \right)^{0.5} \left[\frac{(\rho_l - \rho_g) g \delta^2}{\sigma} \right]^{1/4}$$

Equation A 18

The vapor and liquid velocities are calculated as:

$$v_l = \frac{G(1-x)}{\rho_l (1-\varepsilon)}, v_g = \frac{Gx}{\rho_v \varepsilon}$$

Equation A 19

The liquid Reynolds number in Equation A 12 is calculated from Equation A 20.

$$\mathrm{Re}_l = \frac{4G(1-x)\delta}{(1-\varepsilon)\mu_l}$$

Equation A 20

B. Pressure drop correlations

All the correlations use single-phase expressions for frictional pressure drop, therefore some necessary quantities will be defined first. The single-phase friction factors can be calculated from equations in section 4.3 with the respective Reynolds number. Re_l is calculated from Equation A 1, Re_g from Equation B 1, Re_{lo} from Equation A 11 , and Re_{go} from Equation B 2.

$$\mathrm{Re}_g = \frac{GxD}{\mu_g}$$

Equation B 1

$$\mathrm{Re}_{go} = \frac{GD}{\mu_g}$$

Equation B 2

The single-phase frictional pressure gradients are calculated through the following equations [**20**]. For single-phase gas:

$$\left(\frac{dp_{fric}}{dz}\right)_g = \frac{f_g G^2 x^2}{2D\rho_g}$$

Equation B 3

For single phase liquid:

$$\left(\frac{dp_{fric}}{dz}\right)_l = \frac{f_l G^2 (1-x)^2}{2D\rho_l}$$

Equation B 4

For liquid only:

$$\left(\frac{dp_{fric}}{dz}\right)_{lo} = \frac{f_{lo} G^2}{2D\rho_l}$$

Equation B 5

For gas only:

$$\left(\frac{dp_{fric}}{dz}\right)_{go} = \frac{f_{go} G^2}{2D\rho_g}$$

Equation B 6

Lockhart and Martinelli's correlation:

This is the most used correlation historically [**20**], but its accuracy is limited. It is based on a two-phase pressure drop multiplier. The two-phase pressure drop can either be expressed by the single-phase liquid pressure gradient or the single-phase gas pressure gradient:

$$-\frac{dp_{fric}}{dz} = \phi_g^2 \left(\frac{dp_{fric}}{dz} \right)_g = \phi_l^2 \left(\frac{dp_{fric}}{dz} \right)_l$$

Equation B 7

The pressure drop multipliers is a function of the parameter X^2 defined as:

$$X^2 = \frac{\left(\frac{dp_{fric}}{dz} \right)_l}{\left(\frac{dp_{fric}}{dz} \right)_g}$$

Equation B 8

The two-phase multipliers can then be found by the following equations:

$$\phi_l^2 = 1 + \frac{C}{X} + \frac{1}{X^2}$$

Equation B 9

$$\phi_g^2 = 1 + CX + X^2$$

Equation B 10

Where C is an empirical constant that depends on if the flow is laminar or turbulent. Table B 1 shows the values of C depending on if the gas and/or liquid are turbulent or laminar[**20**].

Liquid	Gas	C
Turbulent	Turbulent	20
Laminar	Turbulent	12
Turbulent	Laminar	10
Laminar	Laminar	5

Table B 1 Values of C in Lockhart and Martinelli frictional pressure drop correlation

Chisholm's correlation:

Chisholm's correlation is based on a liquid only two-phase friction multiplier.

$$-\frac{dp_{fric}}{dz} = \phi_{lo}^2 \left(\frac{dp_{fric}}{dz} \right)_{lo}$$

Equation B 11

Where ϕ^2_{lo} is given by the following expression [**20**]:

$$\phi_{lo}^2 = 1 + (Y^2 - 1)\left[Bx^{(\frac{2-n}{2})}(1-x)^{(\frac{2-n}{2})} + x^{2-n} \right]$$

Equation B 12

n is the power of the single-phase frictional factor relationship (see 4.3) . B is given in Table B 2

B	Y
$\frac{55}{G^{1/2}}$	0<Y<9.5
$\frac{520}{YG^{1/2}}$	9.5<Y<28
$\frac{15000}{Y^2G^{1/2}}$	28<Y

Table B 2 Values of B in Chisholm frictional pressure drop correlation

Where Y is

$$Y^2 = \frac{\left(\frac{dp_{fric}}{dz}\right)_{go}}{\left(\frac{dp_{fric}}{dz}\right)_{lo}}$$

Equation B 13

Friedel's correlation:

Friedel's correlation is also based on the liquid only two-phase friction multiplier, but the friction multiplier is correlated as follows [**20**]:

$$\phi_{lo}^2 = E + \frac{3.24FH}{Fr^{0.045}We^{0.035}}$$

Equation B 14

Where

$$E = (1-x)^2 + \frac{x^2\rho_l f_{go}}{\rho_g f_{lo}}$$

Equation B 15

$$F = x^{0.78}(1-x)^{0.24}$$

Equation B 16

$$H = \left(\frac{\rho_l}{\rho_g}\right)^{0.91} \left(\frac{\mu_g}{\mu_l}\right)^{0.19} \left(1 - \frac{\mu_g}{\mu_l}\right)^{0.7}$$

Equation B 17

The Froude number is defined as:

$$Fr = \frac{G^2}{gD\rho_{tp}^2}$$

Equation B 18

The Weber number is defined as:

$$We = \frac{G^2 D}{\rho_{tp}\sigma}$$

Equation B 19

Where the two-phase density is defined here as:

$$\rho_{tp} = \left(\frac{x}{\rho_g} + \frac{1-x}{\rho_g}\right)^{-1}$$

Equation B 20

Fuchs' correlation:

Fuchs' correlation [**19**] is based on experiments with R-12 and consists of a two-phase enhancement factor [**15**]. The two-phase enhancement factor is defined as:

$$\psi = \frac{\frac{dp}{dz_{fric}} - \left(\frac{dp}{dz_{fric}}\right)_{lo}}{\left(\frac{dp}{dz_{fric}}\right)_{go} - \left(\frac{dp}{dz_{fric}}\right)_{lo}}$$

Equation B 21

The two-phase enhancement factor is generally a function of vapor fraction, Froude-number and density ratio between the liquid and the gas, but for Froude-numbers above 1.45 it is only a function of vapor fraction. The flow is then expected to be annular [**15**]. The equation for the two-phase enhancement factor is:

$$\psi = 6740.331720 * x^{11} - 36759.087741 * x^{10} + 85275.119778 * x^{9}$$
$$-110168.145383 * x^{8} + 87170.939162 * x^{7} - 43797.819250 * x^{6}$$
$$+14021.596088 * x^{5} - 2790.120307 * x^{4} + 324.432076 * x^{3}$$
$$-18.611125 * x^{2} + 2.414768 * x - 0.000141$$

Equation B 22

The equation is not retrieved directly from Fuchs [**19**] because it was not possible to obtain, but it is retrieved through personal communication with Bengt O. Neeraas [**30**].

The data for the experiments are [**15**]:
Pressure: 1.2-2.6 bar
Mass flux: 65-775 kg/m²s
Vapor fraction: 0-1

Corrected Fuchs:
Neeraas [**15**] corrected the correlation by Fuchs from his experiments with propane, propane/methane and propane/ethane. The mass fluxes were in the range of 150-400 kg/m²s, pressures between 12 and 40 bar, and vapor fractions between 0 and 1.

$$\left(\frac{dp}{dz}\right)_{fric} = \left(\frac{dp}{dz}\right)_{fric}^{fuchs} f\left(\frac{\rho_l}{\rho_g}, x\right)$$

Equation B 23

Where the correction function f is

$$f\left(\frac{\rho_l}{\rho_g}, x\right) = 1.0 - \left(1.0 - 0.3g\left(\frac{\rho_l}{\rho_g}\right)\right)h(x)$$

Equation B 24

The density correction is defined through the three following equations:

$$g\left(\frac{\rho_l}{\rho_g}\right) = \frac{1.0}{0.3}, \frac{\rho_l}{\rho_g} > 20$$

Equation B 25

$$g\left(\frac{\rho_l}{\rho_g}\right) = \left(\frac{\rho_l}{\rho_g}\right)^{0.4}, 6.5 \le \frac{\rho_l}{\rho_g} \le 20$$

Equation B 26

$$g\left(\frac{\rho_l}{\rho_g}\right) = 6.5^{0.4}, \frac{\rho_l}{\rho_g} < 6.5$$

Equation B 27

And the vapor fraction correction defined by the following two equations:

$$h(x) = \frac{\sin(\pi x) + \sin(\pi x^3)}{1.69}, x \le 0.725$$

Equation B 28

$$h(x) = 1.0 - \sin\left(\frac{\pi}{2}\left(\frac{x - 0.725}{0.275}\right)^{5x^{7/2}}\right), x > 0.725$$

Equation B 29

C. Test case used in comparisons

A typical well stream is used for comparing HTC and pressure drop correlations. Table C 1 shows tube and flow specifications.

Mass flow [kg/s]	0.3
Di [m]	0.026
P [bar]	100
Tube wall roughness [m]	5.00E-05

Table C 1 Tube and flow specifications for test case

The composition of the fluid is shown in Table C 2 and the phase envelope in Figure C 1.

Component	Comp.	Z
Nitrogen	N2	1
Carbon Dioxide	CO2	3
Methane	C1	75
Ethane	C2	8
Propane	C3	5
I-Butane	IC4	1
N-Butane	NC4	1
I-Pentane	IC5	0.5
N-Pentane	NC5	0.5
Hexane	C6	5

Table C 2 Test fluid composition

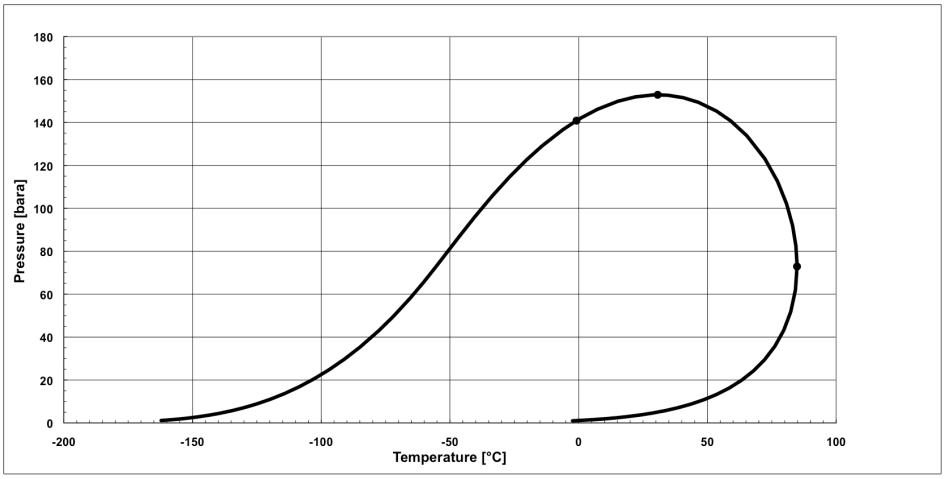

Figure C 1 Phase envelope test fluid

D. MATLAB functions and scripts

Table D 1 shows an overview with description of the different scripts and functions in the calculation model. The scripts for the built-in MATLAB functions are not shown here, but the scripts for the implemented routines are included after the table.

Function	Description
Built-in MATLAB functions	
min(vector)	Returns minimum and position of minimum in vector
max(vector)	Returns maximum and position of maximum in vector
interp1	Interpolates in specified tables
Implemented routines	
twallstart	Returns wall temperature at inlet
hindre	Returns tubeisde HTC in single-phase flow (Gnielinski)
fricsmooth	Return the implicit function for friction factor in smooth tubes (Equation 4.3-5)
hytre	Returns HTC in natural convection around horizontal cylinder
hytref	Returns HTC in forced cross flow over cylinder
hytrekomb	Returns combined natural and forced convection HTC
trykkfall	Returns single-phase friction factor (Haaland)
importfile	Reads to specified file with properties. Importfile is generated by MATLAB
hindreglatt	Return single-phase HTC for smooth tubes (Dittus-Boelter)
hliquid	Returns liquid HTC from HEDH correlation
hliquidboy	Returns liquid HTC from modified Boyko and Kruzhilin correlation
hytrevert	Returns HTC in natural convection around vertical tubes
hytrecocurr	Return HTC in parallel flow over horizontal tubes
lmevoid	Returns void fraction from (Equation A 15-Equation A 17)
fuchscorrected	Returns frictional pressure gradient in two-phase flow (corrected Fuchs correlation)
fuchs	Returns frictional pressure gradient in two-

	phase flow from original Fuchs correlation
euler1naturlig	Solves temperature and pressure profiles in pure natural convection
euler1cocurrent	Solves temperature and pressure profiles in cocurrent parallell flow
euler1crossmixed	Solves temperature and pressure profiles in mixed cross flow
euler1crossunmixed	Solves temperature and pressure profiles in unmixed cross flow
euler1countercurrent	Solves temperature and pressure profiles in countercurrent parallell flow
heatex	m-file where all inlet parameters, tube geometry and water- and tube orientations is chosen. File where properties are located is specified in heatex

Table D 1 MATLAB routines

twallstart

```
function tw1=twallstart(Ti,hi, vsw, teta, l, Tsw,waterorient)
global Do Di k dl hokonst Rf
a=Ti-Tsw;
if hokonst==0
   ho=hytrekomb(a, vsw, teta, l,Tsw,waterorient);
else
   ho=hokonst;
end
htot=1/((1/ho)+Rf+(Do/(hi*Di))+(log(Do/Di)*Do/(2*k)));
hiw=1/((Do/(hi*Di))+Rf+(log(Do/Di)*Do/(2*k)));
sjekk=pi*Do*dl*(htot*(Ti-Tsw)-hiw*(Ti-a));
dt=0.1;
eps=.5;
while ((abs(sjekk)>eps) && (a > Tsw ))
  a=a-dt;
  if hokonst==0
     ho=hytrekomb(a, vsw, teta, l,Tsw,waterorient);
  else
     ho=hokonst;
  end
  htot=1/((1/ho)+Rf+(Do/(hi*Di))+(log(Do/Di)*Do/(2*k)));
  hiw=1/((Do/(hi*Di))+Rf+(log(Do/Di)*Do/(2*k)));
  sjekk=Do*pi*dl*(htot*(Ti-Tsw)-hiw*(Ti-a));
end
tw1=a;
```

hindre

```
function hi=hindre(Re, Pr, Di, l, lambda, fg)
if Re>3000
   f=fzero(@(f) fricsmooth(f, Re), 0.04);
else
   f=64/Re;
end
if (Re>2300) && (Re< 5e4)
   Nusmooth= (f/8)*Re*Pr/(1+ 12.7*(f/8)^(1/2)*(Pr^(2/3)-1));

elseif Re > 5e4
      Nusmooth= (f/8)*Re*Pr/(1+ 12.7*(f/8)^(1/2)*(Pr^(2/3)-1));
else
      Nusmooth=3.66;
end
n=0.68*Pr^0.215;
surfcorr=(fg/f)^n;
Nu=Nusmooth*surfcorr;
hi=Nu*lambda/Di;
```

fricsmooth

```
function g=fricsmooth(f, Re)
g=2.0*log10(Re*f^(1/2))-0.8 - (1/f^(1/2));
```

hytre

```
function ho=hytre(Tw, Tsw)
global Do g
T=5:5:60;
beta=1e-3*[0.015 0.0733 0.138 0.195 0.247 0.294 0.337 0.377 0.415 0.451
0.484 0.517];
Prandtl=[11.2 9.45 8.09 7.01 6.14 5.42 4.83 4.32 3.91 3.55 3.25 2.99];
my=1e-3*[1.519  1.307  1.138  1.002  0.891  0.798  0.720  0.653  0.596  0.547
0.504 0.467];
ro=[999.9 999.9 999.1 998 997 996 994 992.1 990.1 988.1 985.1 983.3];
kond=[0.571 0.580 0.589 0.598 0.607 0.615 0.623 0.631 0.637 0.644 0.649
0.654];
Tf= (Tw+ Tsw)/2;
b=interp1(T, beta, Tf);
Pr=interp1(T, Prandtl, Tf);
u=interp1(T, my, Tf);
p=interp1(T, ro, Tf);
v=u/p;
k=interp1(T, kond, Tf);
```

```
Gr=g*b*(Tw-Tsw)*Do^3/v^2;
Ra=Pr*g*b*(Tw-Tsw)*Do^3/v^2;
Nuf1=(0.518*Ra^(1/4)/(1+(0.559/Pr)^(9/16))^(4/9));
Nuf2=(1+ ((3.47*1e-7*Ra)/(1+(0.559/Pr)^(9/16))^(16/9)))^(1/12);
Nuf= Nuf1*Nuf2;
temp=1+ 2/Nuf;
Nu=2/log(temp);
ho=Nu*k/Do;
```

hytref

```
function hof=hytref(vsw, Tw, Tsw)
global Do
T=5:5:60;
Prandtl=[11.2 9.45 8.09 7.01 6.14 5.42 4.83 4.32 3.91 3.55 3.25 2.99];
my=1e-3*[1.519 1.307 1.138 1.002 0.891 0.798 0.720 0.653 0.596 0.547
0.504 0.467];
ro=[999.9 999.9 999.1 998 997 996 994 992.1 990.1 988.1 985.1 983.3];
kond=[0.571 0.580 0.589 0.598 0.607 0.615 0.623 0.631 0.637 0.644 0.649
0.654];
Tf= (Tw+ Tsw)/2;
Pr=interp1(T, Prandtl, Tf);
u=interp1(T, my, Tf);
p=interp1(T, ro, Tf);
k=interp1(T, kond, Tf);
Re= p*vsw*Do/u;
Nu=                                    0.3                                    +
(0.62*Re^(1/2)*Pr^(1/3)*(1+(Re/282000)^(5/8))^(4/5))/(1+(0.4/(Pr^(2
/3))))^(4/5);
hof= Nu*k/Do;
```

hytrekomb

```
function hokomb=hytrekomb(Tw, vsw, teta,l, Twater,waterorient)
if vsw==0 && teta==0
   hokomb=hytre(Tw, Twater);
   return
elseif vsw==0 && teta==90
   hokomb=hytrevert(Tw, l);
   return
elseif vsw~=0 && (waterorient==2 || waterorient==3)
   hf=hytref(vsw, Tw, Twater);
   if teta==0
      hn=hytre(Tw, Twater);
```

```
    else
      hn=hytrevert(Tw,l);
    end
    hokomb=(hn^4+hf^4)^(1/4);
elseif vsw~=0 && (waterorient==4 || waterorient==5)
    hn=hytre(Tw,Twater);
    hf=hytrecocurr(vsw,Tw,Twater,l);
    hokomb=(hn^4+hf^4)^(1/4);
end
```

trykkfall

```
function f=trykkfall(Re, k, Di)
if Re < 3000
    f=64/Re;
    return
else
    f=(-1.8*log10((6.9/Re)+(k/(3.7*Di))^1.11))^(-2);
end
```

importfile (Generated by MATLAB)

```
function importfile(fileToRead1)
newData1 = importdata(fileToRead1);
vars = fieldnames(newData1);
for i = 1:length(vars)
    assignin('base', vars{i}, newData1.(vars{i}));
end
```

hindreglatt

```
function hi=hindreglatt(Re, Pr, lambda, l)
Nu=0.023*Re^(0.8)*Pr^(0.4);
hi=Nu*lambda/l;
```

hliquid

```
function hl=hliquid(Re, rol, ul, lambdal, cpl, taul)
global g
taupluss=rol*taul/((rol^2*ul*g)^(2/3));
Pr=ul*cpl/lambdal;
m=0.5*(Pr+3);
ny=ul/rol;
if taupluss<=9.04
    Rec= 1600 - 226*taupluss + 0.667*(taupluss^3);
else
    Rec=50;
```

```
end
if Re > Rec
   apluss=((1.41/(Re^0.5))^m                                          +
(0.071*(Pr^0.5)/(Re^(1/24)))^m)^(1/m)*taupluss^(1/2);
else
   apluss=1.41*Re^(-0.5)*taupluss^(0.5);
end
hl=apluss*lambdal*g^(1/3)/(ny^(2/3));
```

hliquidboy

```
function hl=hliquidboy(massfrac, Relo, lambdal, Pr, rol, rog)
global Di ks
f=trykkfall(Relo, ks, Di);
hlo=hindre(Relo,Pr,Di,0,lambdal,f);
hl=(1.15-0.275*massfrac)^(-1)*hlo*(1+ massfrac*((rol/rog)-1))^(0.5);
```

hytrevert

```
function ho=hytrevert(Tw, l)
global Tsw g
T=5:5:60;
beta=1e-3*[0.015 0.0733 0.138 0.195 0.247 0.294 0.337 0.377 0.415 0.451
0.484 0.517];
Prandtl=[11.2 9.45 8.09 7.01 6.14 5.42 4.83 4.32 3.91 3.55 3.25 2.99];
my=1e-3*[1.519 1.307 1.138 1.002 0.891 0.798 0.720 0.653 0.596 0.547
0.504 0.467];
ro=[999.9 999.9 999.1 998 997 996 994 992.1 990.1 988.1 985.1 983.3];
kond=[0.571 0.580 0.589 0.598 0.607 0.615 0.623 0.631 0.637 0.644 0.649
0.654];
Tf= (Tw+ Tsw)/2;
b=interp1(T, beta, Tf);
Pr=interp1(T, Prandtl, Tf);
u=interp1(T, my, Tf);
p=interp1(T, ro, Tf);
v=u/p;
k=interp1(T, kond, Tf);
Ra=Pr*g*b*(Tw-Tsw)*l^3/v^2;
w=(1+(0.492/Pr)^(9/16))^(-16/9);
if Ra<1e9
   Nu=0.503*(Ra*w)^(1/4);
else
   Nu=89.4*Pr^(1/4)*w^(1/4)+0.15*(Ra^(1/3)-1000*Pr^(1/3))*w^(1/3);
end
ho=Nu*k/l;
```

hytrecocurr

```
function ho=hytrecocurr(vsw, Tw, Tsw, x)
T=5:5:60;
Prandtl=[11.2 9.45 8.09 7.01 6.14 5.42 4.83 4.32 3.91 3.55 3.25 2.99];
my=1e-3*[1.519 1.307 1.138 1.002 0.891 0.798 0.720 0.653 0.596 0.547
0.504 0.467];
ro=[999.9 999.9 999.1 998 997 996 994 992.1 990.1 988.1 985.1 983.3];
kond=[0.571 0.580 0.589 0.598 0.607 0.615 0.623 0.631 0.637 0.644 0.649
0.654];
Tf= (Tw+ Tsw)/2;
Pr=interp1(T, Prandtl, Tf);
u=interp1(T, my, Tf);
p=interp1(T, ro, Tf);
k=interp1(T, kond, Tf);
if x==0
   x=0.02;
end
Re=p*vsw*x/u;
Nu=0.0296*Re^(0.8)*Pr^(1/3);
ho=Nu*k/x;
```

lmevoid

```
function e=lmevoid(x,rog,rol,G,sigma)
global g
era=(x/rog)*((1+0.12*(1-x))*((x/rog)+((1-x)/rol))+(1.18*(1-
x)*(g*sigma*(rol-rog)^0.25/(G*rol^0.5))))^(-1);
eh=(1+ ((1-x)/x)*(rog/rol))^(-1);
e= (eh-era)/(log(eh/era));
```

fuchscorrected

```
function dpdz=fuchscorrected(x,G,Relo,Rego,rol,rog)
dpfuchs=fuchs(x,G,Relo,Rego,rol,rog);
densrat=rol/rog;
if densrat>20
   g=1.0/0.3;
elseif (densrat>=6.5) && (densrat < 20)
   g=densrat^(0.4);
else
   g=6.5^(0.4);
end
if x <= 0.725
   h=(sin(pi*x)+sin(pi*x^3))/1.69;
```

```
else
   h=1.0-sin((pi/2)*((x-0.725)/0.275)^(5*x^(7/2)));
end
corr=1.0-(1.0-0.3*g)*h;
dpdz=dpfuchs*corr;
```

fuchs

```
function dpfdl=fuchs(x,G, Relo, Rego, rol, rog)
global Di ks
flo=trykkfall(Relo, ks, Di);
fgo=trykkfall(Rego, ks, Di);
dpldl=flo*G^2/(2*Di*rol);
dpgdl=fgo*G^2/(2*Di*rog);
fuch=6740.331720*x^11-36759.087741*x^10+85275.119778*x^9-
110168.145383*x^8+87170.939162*x^7-
43797.819250*x^6+14021.596088*x^5-
2790.120307*x^4+324.432076*x^3-18.611125*x^2+2.414768*x-
0.000141;
dpfdl=fuch*(dpgdl-dpldl)+dpldl;
```

euler1naturlig

```
global Do Di k ks vsw mtot Tstart Pinn data l mod textdata xtubes
waterorient msw Tsw s hikonst hokonst cpsw Rf g dl
for i=1:length(textdata)
   if strcmp(textdata(i),'Enth (kJ/kg)')==1
      entrow=i;
   elseif strcmp(textdata(i),'Gas molfrac (mol%)')==1
      molfracrow=i;
   elseif strcmp(textdata(i),'Gas massfrac (mass%)')==1
      massfracrow=i;
   elseif strcmp(textdata(i),'Total density (kg/m3)')==1
      totdensrow=i;
   elseif strcmp(textdata(i),'Gas density (kg/m3)')==1
      gasdensrow=i;
   elseif strcmp(textdata(i),'Liquid density (kg/m3)')==1
      liqdensrow=i;
   elseif strcmp(textdata(i),'Gas viscosity (cP)')==1
      gasviscrow=i;
   elseif strcmp(textdata(i), 'Liquid viscosity (cP)')==1
      liqviscrow=i;
   elseif strcmp(textdata(i), 'Gas CP (kj/kgK)')==1
      gascprow=i;
   elseif strcmp(textdata(i), 'Liquid CP (kj/kgK)')==1
```

```
      liqcprow=i;
   elseif strcmp(textdata(i), 'Gas thermal conduc (mW/mC)')==1
      gascondrow=i;
   elseif strcmp(textdata(i), 'Liquid thermal conduc (mW/mC)')==1
      liqcondrow=i;
   elseif strcmp(textdata(i), 'Oil/gas interfacial tension (mN/m)')==1
      surftensrow=i;
   end
end
g=9.81;
n=round(l/dl);
dA=pi*Do*l/n;
T=zeros(xtubes,n);
Tw=zeros(xtubes,n);
Twater=zeros(1, xtubes);
for yt=1:xtubes
   Twater(yt)=Tsw;
end
m=zeros(1,xtubes);
dampfrac=zeros(1,xtubes);
P=T;
htottab=T;
hitab=T;
hwtab=T;
hiwtab=T;
hutside=T;
friksjon=T;
Reynold=T;
x=T;
Prandtl=T;
trykktap=m;
dp=0;
dm=0;
for ror=1:xtubes
   m(ror)=mtot/xtubes;
end
[dpmin,jmin]=min(trykktap);
[dpmax, jmax]=max(trykktap);
while (deltadp>1e-2*dpmax) || (trykktap(1)==0)
   if (trykktap(1))~=0
      dm=(deltadp/2)^(1/2)*Di^2/l;
      m(jmax)=m(jmax)-dm;
      m(jmin)=m(jmin)+dm;
```

```
end
Qtot=0;
for j=1:xtubes
   G=m(j)*4/(pi*Di^2);
   T(j,1)=Tstart;
   ro=interp1(data(1,:),data(gasdensrow,:), T(j,1),'spline');
   u=(interp1(data(1,:),data(gasviscrow,:), T(j,1),'spline'))/1000;
   cp=(interp1(data(1,:),data(gascprow,:), T(j,1),'spline'))*1000;
   lambda=(interp1(data(1,:),data(gascondrow,:), T(j,1),'spline'))/1000;
   Pr= u*cp/lambda;
   molfrac=(interp1(data(1,:),data(molfracrow,:), T(j,1)))/100;
   massfraci=(interp1(data(1,:),data(massfracrow,:), T(j,1)))/100;
   ul=(interp1(data(1,:), data(liqviscrow,:), T(j,1), 'spline'))/1000;
   rol=interp1(data(1,:), data(liqdensrow,:), T(j,1),'spline');
   lambdal=(interp1(data(1,:),data(liqcondrow,:), T(j,1),'spline'))/1000;
   cpl=(interp1(data(1,:),data(liqcprow,:), T(j,1),'spline'))*1000 ;
   sigma=(interp1(data(1,:), data(surftensrow,:), T(j,1), 'spline'))/1000;
   Prl=ul*cpl/lambdal;
   if isnan(massfraci)==1
      massfraci=1;
   elseif massfraci>0.99 && massfraci<1
      massfraci=.99;
   end
   if massfraci==1
      v=m(j)/(ro*(pi*Di^2/4));
      Re=ro*v*Di/u;
      f=trykkfall(Re, ks, Di);
      if mod~=4
         hi=hindre(Re, Pr, Di, l, lambda,f);
      elseif mod==4
         hi=hikonst;
      end
   elseif (massfraci<=1) && (massfraci>=0)
      entalp1=(interp1(data(1,:),data(entrow,:), (T(j,1)+.5),'spline'))*1000;
      entalp2=(interp1(data(1,:),data(entrow,:), T(j,1),'spline'))*1000;
      dtdh=((T(j,1)+.5)-Tstart)/(entalp1-entalp2);
      zg=massfraci*cp*dtdh;
      mliq=abs(m(j)*(1-massfraci));
      e1=lmevoid(massfraci,ro,rol,G,sigma);
      delta=Di/2- (e1*Di^2)^(1/2)/2;
      Rel=4*G*(1-massfraci)*delta/((1-e1)*ul);
      Relo=G*Di/ul;
      Rego=G*Di/u;
```

```
    dpfdl=fuchscorrected(massfraci, G, Relo, Rego, rol, ro);
    vgs=G*massfraci/ro;
    Regs=ro*vgs*Di/u;
    vg=G*massfraci/(ro*e1);
    Re=ro*vg*Di/u;
    vl=G*(1-massfraci)/(rol*(1-e1));
    fgs=trykkfall(Regs, ks, Di);
    if mod~=4
      if mod==2
        hliq=hliquidboy(massfraci, Relo, lambdal, Prl, rol, ro);
        dpfgsdl=trykkfall(Regs, ks, Di)*ro*vgs^2/(2*Di);
        cf=(dpfdl/dpfgsdl)^0.445;
        hg=cf*hindreglatt(Re, Pr, lambda, Di);
      elseif mod==1
        taui=dpfdl*Di/4;
        hliq= hliquid(Rel, rol, ul, lambdal, cpl, taui);
        dpfgsdl=trykkfall(Regs, ks, Di)*ro*vgs^2/(2*Di);
        cf=(dpfdl/dpfgsdl)^0.445;
        hg=cf*hindreglatt(Re, Pr,lambda,Di);
      else
        fi=1+ (vg/vl)^(0.5)*((rol-ro)*g*delta^2/sigma)^(1/4);
        hliq=0.003*Rel^0.74*Prl^0.5*lambdal*fi/delta;
        hg=fi*hindreglatt(Re, Pr, lambda, Di);
      end
      hi=1/((1/hliq)+(zg/hg));
    elseif mod==4
      hi=hikonst;
    end
  elseif massfraci==0
    v=m(j)/(rol*(pi*Di^2/4));
    Rel=rol*v*Di/ul;
    f=trykkfall(Rel, ks, Di);
    if mod~=4
      hi=hindre(Rel, Prl, Di, l, lambdal,f);
    elseif mod==4
      hi=hikonst;
    end
  end
  P(j,1)=Pinn;
  Q=0;
  dpftp=0;
  dpfsp=0;
  dpa=0;
```

```
    dph=0;
    dphdl=0;
    x(1)=0;
    Tw(j,1)=twallstart(T(j,1), hi, vsw,teta, (x(1)+dl),
Twater(j),waterorient);
    dp=0;
    for i=1:(n)
      x(i+1)=x(i)+dl;
      if hokonst==0
        ho=hytrekomb(Tw(j,i), vsw, teta, x(i+1), Twater(j),waterorient);
      else
        ho=hokonst;
      end
      hutside(j,i)=ho;
      ro=interp1(data(1,:),data(gasdensrow,:), T(j,i),'spline');
      u=(interp1(data(1,:),data(gasviscrow,:), T(j,i),'spline'))/1000;
      cp=(interp1(data(1,:),data(gascprow,:), T(j,i),'spline'))*1000;
      lambda=(interp1(data(1,:),data(gascondrow,:), T(j,i),'spline'))/1000;
      ul=(interp1(data(1,:), data(liqviscrow,:), T(j,i), 'spline'))/1000;
      rol=interp1(data(1,:), data(liqdensrow,:), T(j,i),'spline');
      lambdal=(interp1(data(1,:),data(liqcondrow,:), T(j,i),'spline'))/1000;
      cpl=(interp1(data(1,:),data(liqcprow,:), T(j,i),'spline'))*1000 ;
      sigma=(interp1(data(1,:), data(surftensrow,:), T(j,i), 'spline'))/1000;
      Pr= u*cp/lambda;
      Prl=ul*cpl/lambdal;
      massfrac=(interp1(data(1,:),data(massfracrow,:), T(j,i)))/100;
      if isnan(massfrac)==1
        massfrac=1;
      end
      hwtab(j,i)=2*k/(Do*log(Do/Di));
      if massfrac==1
        v=m(j)/(ro*(pi*Di^2/4));
        Re=ro*v*Di/u;
        f=trykkfall(Re, ks, Di);
        if mod~=4
          hi=hindre(Re, Pr, Di, l, lambda,f);
        elseif mod==4
          hi=hikonst;
        end
        h= 1/((1/ho)+Rf+(Do/(hi*Di))+(log(Do/Di)*Do/(2*k)));
        hiw=1/((Do/(hi*Di))+Rf+(log(Do/Di)*Do/(2*k)));
        T(j,i+1)=T(j,i)+ dA*h*(Twater(j)-T(j,i))/(m(j)*cp);
        Tw(j,i+1)=T(j,i) - (h/hiw)*(T(j,i)-Twater(j));
```

```
            dQ=m(j)*cp*(T(j,i)-T(j,i+1));
            dpfdl= f*v^2*ro/(2*Di);
            ro2=interp1(data(1,:),data(gasdensrow,:), T(j,i+1),'spline');
            dpadl=-G^2*((1/ro2)-(1/ro));
            if teta==90
               dphdl=(ro+ro2)*g/2;
               dph=dph+ dphdl*dl;
            end
            dpa=dpa+dpadl;
            dpfsp=dpfsp+dpfdl*dl;
            P(j,i+1)=P(j,i)-dpfdl*dl/1e5 + dpadl/1e5-dphdl*dl/1e5;
            hitab(j,i)=hi;
            hiwtab(j,i)=hiw;
            htottab(j,i)=h;
         elseif massfrac<1 && massfrac>0
            entalp1=(interp1(data(1,:),data(entrow,:), T(j,i),'spline'))*1000;
            if i>1
               entalp2=(interp1(data(1,:),data(entrow,:),                T(j,i-
1),'spline'))*1000;
               dtdh=(T(j,i)-T(j,i-1))/(entalp1-entalp2);
               zg=massfrac*cp*dtdh;
            end
            mliq=abs(m(j)*(1-massfrac));
            e1=lmevoid(massfrac,ro,rol,G,sigma);
            delta=Di/2- (e1*Di^2)^(1/2)/2;
            vg=G*massfrac/(ro*e1);
            vl=G*(1-massfrac)/(rol*(1-e1));
            vgs=G*massfrac/ro;
            Re=ro*vg*Di/u;
            Rel=4*G*(1-massfrac)*delta/(ul*(1-e1));
            Relo=G*Di/ul;
            Rego=G*Di/u;
            Regs=ro*vgs*Di/u;
            dpfdl=fuchscorrected(massfrac, G, Relo, Rego, rol, ro);
            fgs=trykkfall(Regs, ks, Di);
            if mod~=4
               if massfrac<0.95
                  if mod==1
                     dpfgsdl=trykkfall(Regs, ks, Di)*ro*vgs^2/(2*Di);
                     cf=(dpfdl/dpfgsdl)^0.445;
                     taui=dpfdl*Di/4;
                     hliq= hliquid(Rel, rol, ul, lambdal, cpl, taui);
                     hg=cf*hindreglatt(Re, Pr, lambda,Di);
```

```
            elseif mod==2
              hliq=hliquidboy(massfrac, Relo, lambdal, Prl, rol, ro);
              dpfgsdl=fgs*ro*vgs^2/(2*Di);
              cf=(dpfdl/dpfgsdl)^0.445;
              hg=cf*hindreglatt(Re, Pr, lambda, Di);
            elseif mod==3
              fi=1+ (vg/vl)^(0.5)*((rol-ro)*g*delta^2/sigma)^(1/4);
              hliq=0.003*Rel^0.74*Prl^0.5*lambdal*fi/delta;
              hg=fi*hindreglatt(Re, Pr, lambda, Di);
            end
            heff=1/((1/hliq)+(zg/hg));
          elseif massfrac>0.95
            heff=hindre(Regs,Pr,Di,l,lambda,fgs);
          end
        elseif mod==4
          heff=hikonst;
        end
        h= 1/((1/ho)+Rf+(Do/(heff*Di))+(log(Do/Di)*Do/(2*k)));
        dQ=h*dA*(T(j,i)-Twater(j));
        entalp=entalp1*m(j)-dQ;
        hiw=1/((Do/(heff*Di))+Rf+(log(Do/Di)*Do/(2*k)));
        T(j,i+1)=interp1(data(entrow,:),                    data(1,:),
entalp/(m(j)*1000),'spline');
        Tw(j,i+1)=T(j,i) - (h/hiw)*(T(j,i)-Twater(j));
        ro2=interp1(data(1,:),data(gasdensrow,:), T(j,i+1),'spline');
        rol2=interp1(data(1,:), data(liqdensrow,:), T(j,i+1),'spline');
        massfrac2=(interp1(data(1,:),data(massfracrow,:), T(j,i+1)))/100;
        e2=lmevoid(massfrac2,ro2,rol2,G,sigma);
        if teta==90
          dphdl=((ro+ro2)*(e1+e2)/4 + ((rol+rol2)/2)*(1 - (e1+e2)/2))*g;
          dph=dph+ dphdl*dl;
        end
        dpadl=-G^2*((massfrac2^2/(e2*ro2))+        ((1-massfrac2)^2/((1-
e2)*rol2)) - ((massfrac^2/(e1*ro))+ ((1-massfrac)^2/((1-e1)*rol))));
        dpa=dpa+dpadl;
        dpftp=dpftp+dpfdl*dl;
        hitab(j,i)=heff;
        htottab(j,i)=h;
        P(j,i+1)=P(j,i)-dpfdl*dl/1e5+dpadl/1e5-dphdl*dl/1e5;
      elseif massfrac==0
        v=m(j)/(rol*(pi*Di^2/4));
        Re=rol*v*Di/ul;
        f=trykkfall(Rel, ks, Di);
```

```
            if mod~=4
               hi=hindre(Rel, Pr, Di, l, lambdal,f);
            elseif mod==4
               hi=hikonst;
            end
            h= 1/((1/ho)+(Do/(hi*Di))+(log(Do/Di)*Do/(2*k)));
            hiw=1/((Do/(hi*Di))+(log(Do/Di)*Do/(2*k)));
            T(j,i+1)=T(j,i)+ dA*h*(Twater(j)-T(j,i))/(m(j)*cpl);
            Tw(j,i+1)=T(j,i) - (h/hiw)*(T(j,i)-Twater(j));
            dQ=m(j)*cpl*(T(j,i)-T(j,i+1));
            dpfdl= f*v^2*rol/(2*Di);
            ro2l=interp1(data(1,:),data(liqdensrow,:), T(j,i+1),'spline');
            dpadl=-G^2*((1/ro2l)-(1/rol));
            dpa=dpa+dpadl;
            dpfsp=dpfsp+dpfdl*dl;
            P(j,i+1)=P(j,i)-dpfdl*dl/1e5 - dpadl/1e5;
            hitab(j,i)=hi;
            hiwtab(j,i)=hiw;
            htottab(j,i)=h;
         end
         dp=dp+dpfdl*dl-dpadl+dphdl*dl;
         Q=Q+dQ;
      end
      trykktap(j)=dp;
      dampfrac(j)=massfrac;
      Qtot=Qtot+Q;
   end
   [dpmin,jmin]=min(trykktap);
   [dpmax, jmax]=max(trykktap);
end
deltaH=interp1(data(1,:),data(entrow,:),Tstart,'spline')*mtot*1000-Qtot;
Tout=interp1(data(entrow,:), data(1,:),deltaH/(mtot*1000));
massfracout=interp1(data(1,:),data(massfracrow,:), Tout)/100;
deltaP=mean(trykktap)/1e5;
output.Duty_kW=Qtot/1e3;
output.T_out=Tout;
output.Pressure_loss_Bar=deltaP;
output.Outer_Area_m2=pi*Do*l*xtubes;
output.Mass_fraction=massfracout;
disp(output)
x=0:dl:l;
figure(1)
ji=plot(x,T(1,:),x, Tw(1,:));
```

```
grid on
xlabel('z [m]')
ylabel('T [C]')
legend('Tube', 'Wall');
set(ji,'LineWidth',2.5)
figure(2)
x2=0:dl:(l-dl);
gi=plot(x2, hitab(1,:), x2, hutside(1,:), x2, htottab(1,:));
grid on
xlabel('z [m]')
ylabel(' HTC [W/m2K]')
legend('Tubeside HTC', 'Waterside HTC', 'Overall HTC');
set(gi,'LineWidth',2.5)
```

euler1cocurrent

Similar to *euler1naturlig*, but with the following additional lines for updating the water temperature. Small font illustrates existing code.

```
        ....
        htottab(j,i)=h;
    end
        Twater(j,i+1)=Twater(j,i) + dQ/(msw*(1/xtubes)*cpsw);
        ...
```

euler1crossmixed

Similar to *euler1naturlig*, but with the following additional lines for updating the water temperature:

```
        ...
  dampfrac(j)=massfrac;
   if j<xtubes
     Twater(j+1)=Q/(msw*cpsw) + Twater(j);
   end
        ...
```

euler1crossunmixed

Similar to *euler1naturlig*, but with the following additional lines for updating the water temperature:

```
        ...
htottab(j,i)=h;
    end
      if j<xtubes
          Twater(j+1,i)=Twater(j,i) + dQ/(msw*(dl/l)*cpsw);
      end
        ...
```

euler1countercurrent

Similar to *euler1cocurrent*, but with an additional *while*-loop for the determining the seawater temperature at the inlet:

...

```
for j=1:xtubes
        Tswguess=Tsw+5;
        Tswend=0;
        while (abs(Tswend-Tsw))>0.5
            .....
            Qtot=Qtot+Q;
            Tswend=Twater(j,i);
            tempdiff=abs(Tswend-Tsw);
           dT=tempdiff*0.5;
           if Tswend < Tsw
               Tswguess= Tswguess+dT;
        elseif Tswend > Tsw
              Tswguess=Tswguess-dT;
          end
        end
        ...
```

heatex

```
clear all
global Do Di k ks vsw mtot Tstart Pinn data l mod textdata xtubes
waterorient msw Tsw s hikonst hokonst cpsw Rf
s = warning('off', 'all');
%Tube spesifications
Do=0.0603;
veggtykkelse=0.00391;
Di=Do- 2*veggtykkelse;
l=220;
k=15; %Tube thermal conductivity
ks=0.002e-3; %Tube wall roughness
xtubes=1;   %NUmber of tubes
teta=0;
%Inlet conditions
Tstart=80;
mtot=1;    %total mass flow
Pinn=100; %inlet pressure

%Step size
dl=0.04;
%Waterside flow
% 1 for natural convection, 2 for cross flow mixed,3 for cross flow unmixed,
4 for cocurrrent, 5 for
% countercurrent
waterorient=1;
Tsw=5;
```

```
%Fouling resistance
Rf=0;

Atot=Do*pi*l*xtubes;
rosw=1000;
cpsw=4200;
if waterorient==1
   vsw=0;
elseif waterorient==2 || waterorient==3
   msw=Inf;
   vsw=0.6;
elseif waterorient==4 || waterorient==5
   msw=Inf;
   vsw=1;
end
%file with properties
importfile('gas100.csv')
data;
textdata;
%Correlation for HTC in condesing: 1 for HEDH, 2 for Boyko &
%Kruzshuilin, 3 for thome 4 for konst
mod=2;

if mod==4
   hikonst=1000; %Constant tube-side HTC
end

%Hokonst equal to zero if not used. if desirable with constant outer HTC
%set hokonst to desired value
hokonst=0;

if waterorient==1
   euler1naturlig
elseif waterorient==2
   euler1crossmixed
elseif waterorient==3
   euler1crossunmixed
elseif waterorient==4
   euler1cocurrent
elseif waterorient==5
   euler1countercurrent
end
```